



HAL
open science

Achieving small-world properties using bio-inspired techniques in wireless networks

Rachit Agarwal, Abhik Banerjee, Vincent Gauthier, Monique Becker, Chai Kiat Yeo, Bu Sung Lee

► **To cite this version:**

Rachit Agarwal, Abhik Banerjee, Vincent Gauthier, Monique Becker, Chai Kiat Yeo, et al.. Achieving small-world properties using bio-inspired techniques in wireless networks. *The Computer Journal*, 2012, 55 (8), pp.909-931. 10.1093/comjnl/bxs024 . hal-00724432

HAL Id: hal-00724432

<https://hal.science/hal-00724432>

Submitted on 21 Aug 2012

HAL is a multi-disciplinary open access archive for the deposit and dissemination of scientific research documents, whether they are published or not. The documents may come from teaching and research institutions in France or abroad, or from public or private research centers.

L'archive ouverte pluridisciplinaire **HAL**, est destinée au dépôt et à la diffusion de documents scientifiques de niveau recherche, publiés ou non, émanant des établissements d'enseignement et de recherche français ou étrangers, des laboratoires publics ou privés.

Achieving Small World Properties using Bio-Inspired Techniques in Wireless Networks

Rachit Agarwal*, Abhik Banerjee*[†], Vincent Gauthier*, Monique Becker*, Chai Kiat Yeo[†] and Bu Sung Lee[†]

*Lab. CNRS SAMOVAR UMR 5157, Telecom Sud Paris, Evry, France

Email: {rachit.agarwal, vincent.gauthier, monique.becker}@telecom-sudparis.eu

[†] CeMNet, School of Computer Engineering, Nanyang Technological University, Singapore

Email: {abhi0018, asckyeo, ebslee}@ntu.edu.sg

Abstract—It is highly desirable and challenging for a wireless ad hoc network to have self-organization properties in order to achieve network wide characteristics. Studies have shown that Small World properties, primarily low average path length and high clustering coefficient, are desired properties for networks in general. However, due to the spatial nature of the wireless networks, achieving small world properties remains highly challenging. Studies also show that, wireless ad hoc networks with small world properties show a degree distribution that lies between geometric and power law. In this paper, we show that in a wireless ad hoc network with non-uniform node density with only local information, we can significantly reduce the average path length and retain the clustering coefficient. To achieve our goal, our algorithm first identifies logical regions using Lateral Inhibition technique, then identifies the nodes that beamform and finally the beam properties using Flocking. We use Lateral Inhibition and Flocking because they enable us to use local state information as opposed to other techniques. We support our work with simulation results and analysis, which show that a reduction of up to 40% can be achieved for a high-density network. We also show the effect of *hopcount* used to create regions on average path length, clustering coefficient and connectivity.

Index Terms—autonomous communication, Complex Networks, Small World properties, Beamforming, Bio-Inspired, Lateral Inhibition, Flocking, Centrality, autonomous communication, Complex Networks, Small World properties, Beamforming, Bio-Inspired, Lateral Inhibition, Flocking, Centrality

I. INTRODUCTION

Decades of academic and industrial research in wireless networks [1] has led to the tremendous growth of wireless networks requiring researchers to address manageability and scalability issues. Due to these issues, most of the research work has been oriented towards autonomous wireless networks. The autonomous behavior of the wireless nodes made decentralized computing and cost efficient topology deployment possible [2]. It was also proved that self-organization of the network can lead to better performance.

An attractive model to achieve better network performance is the Small World network. Small world networks are characterized by reduced Average Path Length (*APL*) and high Clustering Coefficient (*CC*). Here, the *APL* is the mean of *hopcount* between all pairs of nodes in the network. Consider a node, v , with k neighbors. In the sub-graph of these $k + 1$ nodes, the *CC* is defined as the fraction of links that exist to the maximum number of links that could have existed in the sub-graph. Drawing inspiration from the experimental work of Stanley Milgram [3], Watts et al [4] proposed a model that could achieve small world properties. In the model, Watts et al proposed, small world properties could be reached by randomly rewiring a few existing links within the network. Watts et al

showed that the dynamics of these small world networks lie between that of a regular network and a random network [4], [5]. To prove the findings, however, Watts et al used a regular wired network and called the rewired links as shortcuts. Many complex real world networks such as internet, biological networks, food web and social networks also demonstrate small world properties [6], [7], [8]. In real world networks where there is a non-uniform distribution of nodes, these real world networks were shown to exhibit the properties of scale-free networks marked by power law degree distribution. Section VI-A provides more details on small world networks.

In a wireless ad hoc network, achieving small world properties can help us in many ways. Having a low *APL* would increase the performance of the network in terms of communication [9], [10] (reduced traffic per unit area, reduced congestion and reduced signal interference), low latency and reduce the overall energy consumption in the network during the data communication. On the other hand, maintaining the *CC* would ensure connectivity to the neighborhood and would make the network resilient [11], [12]. However, Watts' model cannot be applied directly to wireless ad hoc networks because of the spatial nature of such networks. In wireless ad hoc networks, addition of a shortcut between any two nodes should depend on the distance between two nodes. Helmy in [13] first studied the effect of adding few distance-limited links in the network. He showed that, upon introduction of distance-limited links, wireless ad hoc networks show small world properties. He concluded that, when the shortcut lengths are $\frac{1}{4}$ th of the network diameter, there is a maximum reduction in the *APL*. Thus, proving that realization of small world properties in a wireless ad hoc network depends crucially on the length of shortcuts created among nodes. Another important factor in the realization of small world properties is the choice of nodes among which shortcuts are to be created. One method to obtain these nodes is that of *preferential attachment* [14], [7], typically observed in real world networks, wherein links are created to nodes with high structural importance. It was shown that, analogous to real world networks, using *preferential attachment* for creation of distance-limited links in a spatial network resulted in reduced network diameter [15], [16]. This was accompanied by high clustering coefficient and a shift in the node degree distribution towards power law. These results motivate us to say that, creation of links to nodes having high structural importance in the network can result in the desired small world characteristics.

The creation of a wireless ad hoc network with the small world properties also depends on the manner in which distance-limited links are added. Such links can be added through different techniques like: 1) creating the directional beam using the same power as when the node was operating in the omnidirectional mode; 2) increasing the omnidirectional transmission range of the node; 3) introducing of few long wired links [17]; 4) introducing special nodes with higher omnidirectional transmission range

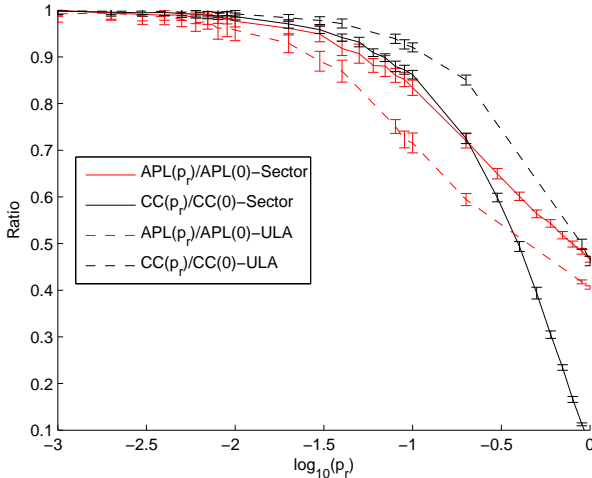


Fig. 1. Source: [18], Effect of beamforming on the APL and the CC when the nodes are using 1) Sector model and 2) ULA Model. The results obtained show a reduction in the APL while almost no change in the CC for the case when we use a realistic antenna model. On the other hand, for the theoretical model, the reduction in the APL is relatively less while the reduction in CC is considerably large. The number of nodes that beamform is shown with a probability value in the log scale. The results also show that the reduction in the APL increases with an increase in the number of beamforming nodes, [4], [5]. Here, $APL(p_r)$ and $CC(p_r)$ are the APL and the CC of the network when $p_r\%$ of the nodes create long-range links. $p_r = 0$ means no node is beamforming. Further, in the figure, we normalize $APL(p_r)$ and $CC(p_r)$ to account for the variation in the APL and the CC .

deterministically in the network [12]; 5) using another antenna for beamforming in addition to the omnidirectional antenna.

Talking about the self-organization characteristics of the nodes, only techniques one and two mentioned above qualify. However, even though other techniques help in achieving desired network characteristics, they lack self-organization capabilities. In addition, the second technique suffers from the problem of early death of the node due to increased energy consumption. Thus leaving us only the first technique. Achieving reorganization or rewiring in a wireless ad hoc network through the first technique is hard due to the spatial nature of the wireless ad hoc network. Finding the beam direction, the beam length and determining the new neighborhood are primary issues associated with rewiring in a wireless ad hoc network. Our previous study, [18], proved that the use of distance-limited long links in wireless ad hoc network to achieve small world properties is beneficial. (Cf. Fig. 1).

Motivated by this, in this study, we investigate how we can increase connectivity, reduce the APL and almost maintain the CC in a non-uniformly distributed wireless ad hoc network. We thus propose an algorithm that achieves these goals by creating long-range directional beams between nodes that have low and high structural importance. The decentralized computing and self-organizing requirements of such an approach motivate us to draw inspirations from nature. We further propose that Lateral Inhibition [19], [20], [21], [22] and Flocking [23], in conjunction with the centrality concept of graph theory, can provide valuable insights in building a solution to our problem.

We use Lateral Inhibition to create small logical regions within a network. The use of Lateral Inhibition not only reduces the message complexity but also enables us to apply the Flocking rule analogy successfully. We use analogy of Flocking rules to identify the nodes that beamform and the beam properties. According to the rules, explained later in section VI-D, it is important to identify stray nodes, align the nodes and move them towards the centroid of their neighborhood. Analogous to this, after

region formation in a non-uniformly distributed wireless ad hoc network, we use Flocking rules to identify the beamforming nodes and direct the beams of these beamforming nodes towards the centroid of the region. The centroid node in the region has a high structural importance. Beamforming towards the centroid node of the region contributes towards reducing the APL because the centroid node of the region is the most connected node and has the highest Closeness Centrality measure. Thus, beamforming towards the centroid node is the *preferential attachment* behavior of the beamforming node, thereby making centroid finding a prerequisite to Flocking. In a distributed system where nodes only have local information and lack GPS facilities, exact centroid node identification of the region is challenging. We can only make an estimate to the centroid node location in the region. We, therefore, use the self-organizing virtual coordinate scheme combined with the centrality concepts to identify the centroid nodes.

Thus, our algorithm design is such that it first identifies regions using Lateral Inhibition, then identifies the centroid nodes of the regions and then uses the analogy of flocking rules to identify the nodes that will beamform along with their beam properties. Section II gives a formal description of our proposed algorithm.

The organization of rest of this paper is as follows. Section II presents the assumptions used for the proposed algorithm along with the algorithm specifications. Section III presents the formal definitions. Section IV and V discuss the simulation setup and the results respectively. For the readers who are unfamiliar with the concepts used in this paper, we provide a detailed description of the same in section VI. We finally conclude our work in the section VIII after providing insights to some future research directions in section VII.

II. ASSUMPTIONS AND ALGORITHM

A. Assumptions

To address issues mentioned in the Introduction, we focus ourselves towards the deployment of homogenous and autonomous wireless ad hoc nodes with no central entity controlling the nodes. This type of deployment enables us to easily apply self-organizing features, achieve global consensus with very limited local information, make any eligible node the group leader, make the system highly fault tolerant, ease the topological maintenance, lower the deployment cost and extend to incorporate the mobility of the nodes in the future. Further, the nodes are set to have an omnidirectional transmission range r . We assume a non-uniform distribution of nodes generated using thinning process defined by Bettstetter et al [24]. The non-uniform distribution of nodes allows us to realize scenarios that are more realistic. The algorithm proposed by Bettstetter et al proceeds by removing nodes which have less than ℓ_{min} neighbors within a transmission range r_b (ref. section VI-F). Further, we assume the deployment of the nodes on a 2-D plane of area A .

As part of our network setup, our algorithm assumes each node to have an antenna consisting of M isotropic elements. The use of single antenna element results into omnidirectional beam while use of more than one antenna element results into a long-range directional beam. A node, however, decides to use more than one antenna element using simple local rules mentioned later in this section. The nodes use beamforming only to transmit data but use omnidirectional beams for reception. We have used the Sector model¹ [25] to visualize our algorithm and have assumed transmission of data to be synchronous.

Further, we assume that the nodes lack GPS facilities and global network knowledge. To achieve our goal, it is thus first essential to know what information can be used by the nodes. We limit a node to use local information along with that of its one hop neighborhood. Determining single hop neighborhood

¹Sector model approximates realistic antenna models

to build the local information is thus essential for the correct operation of the algorithm. Various studies have proposed many neighborhood discovery mechanisms, eg. [26], and have carefully analyzed them. Therefore, for our approach, we assume that all the nodes have information about their neighborhood.

It is also essential to address the self-organizing paradigms, [27], to claim for the self-organizing behavior of the network. Prehofer et al's [27] paradigms state: designing local rules to achieve global properties, implicit coordination, minimizing the use of historic information about the state of the network and designing an algorithm that changes with environment parameters. Our algorithm uses only locally available information to determine the beamforming nodes, beam properties and the regions. The nodes implicitly coordinate with their neighbors to determine the node with the highest *hopcount* from the centroid of the region. For a given region, the nodes also coordinate implicitly to determine the centroid node of that region. The current discussion focuses on a static network. In dynamic network scenarios, optimizing the extent of reconfiguration to deal with frequent changes in state information is likely to be a crucial factor. We leave this for future investigation but offer some insights in section VII.

We further describe the system model and the algorithm in the following sections.

B. System Model

Given a network, $G(V, E)$, where V is the set of vertices and E is the set of edges, we visualize G as a network consisting of N logical regions, $\{G_1, G_2, \dots, G_N\}$, i.e., $G = \bigcup_{i=1}^N G_i$. Each region, G_i , consists of the set of nodes, $V_i | V_i \subset V$ and $V = \bigcup_{i=1}^N V_i$, and set of edges, $E_i | E_i \subset E$ and $E = \bigcup_{i=1}^N E_i$. All vertices in G_i are located within g hops of a head node, h_i . As a part of our algorithm, we use Lateral Inhibition to identify regions and regional heads.

We characterize the set of vertices, V , into three sets. These are termed as the Peripheral node set, the Centroid node set and the Standard node set. We provide separate role to the nodes in these sets. The Peripheral nodes set (P) contains the nodes that beamform. The Centroid node set (C) contains the nodes towards which the nodes in the Peripheral node set beamform. We call the set of remaining nodes, $S = V - (P \cup C)$, as the Standard node set. Further, we call nodes in these sets as the peripheral nodes, the centroid nodes and the standard nodes respectively.

Mathematically, Closeness centrality of a node, $v \in V$, in a graph G is equal to $\frac{1}{\sum_{w \in V} hops(v, w)}$, where $hops(v, w)$ is the *hopcount* between nodes v and w . The node having maximum Closeness Centrality is the centroid of the graph and has a high structural importance. For the vertex sets defined above, nodes in the set P have lowest value of Closeness Centrality, i.e., $\arg \max_{v \in V} \{\sum_{w \in V, v \neq w} hops(v, w)\}$. However, the nodes in the set C have highest value of closeness centrality, i.e., $\arg \min_{v \in V} \{\sum_{w \in V, v \neq w} hops(v, w)\}$. A node in P beamforms towards a node in C in order to minimize the distance to other nodes and reduce *APL*.

The directional beam is modeled using Sector model, i.e., for a given directional beam length B_l , the corresponding beam width, B_w , is

$$B_w = \frac{2\pi r^2}{B_l^2} \quad (1)$$

In realistic antenna model, as beam length of the directional antenna is dependent on the number of antenna elements used, m , the corresponding value of B_l used is $B_l = m * r$.

Further, table I lists the notations used in this paper.

C. Algorithm

We divide our approach into two parts:

- A) Use of Lateral Inhibition technique and self-organizing virtual coordinate scheme for the identification of regions and the centroid nodes of the regions, so that there are less message overheads and nodes can beamform towards the centroid node to achieve reduced *APL*. Section II-C1 provides more details.
- B) Use of flocking rules to identify the nodes that beamform, to determine beam properties that realize small world properties and improve connectivity. Section II-C2 provides more details.

We describe these parts in detail in the next sub sections.

1) *Region formation and Centroid finding*: The Closeness Centrality [28], [29] identifies the structural importance of the node in the network. The node with the highest Closeness Centrality value is the most central node in the network. Through this node, the spread of the information to other nodes is quick. To determine the Closeness Centrality of the node, the node requires the knowledge of other nodes in the region as suggested by the definition of Closeness Centrality, (ref. section VI-E3). This makes the Closeness Centrality a global measure. Storing information about all the nodes in the network can consume a lot of node's memory. When there is lack of global information, gathering such information can also be time consuming and the message complexity could be high. To overcome these problems, we create small logical regions. The creation of regions not only reduces the message complexity of the network but also reduces the effect on the *APL* due to the failure of a node, thereby making the network more manageable, efficient and tolerant to failures [30]. Some algorithms designed in this direction were centralized. The Base Station chose the region heads based on the energy and the position of the nodes. Other techniques use either the transmission power or the degree or the mobility, eg., *WACA* [31]. On the contrary to centralized approaches, some algorithms were either distributed, [32], or probabilistic [33].

We thus divide this part into two, identification of regions using Lateral Inhibition and identification of centroid node in the region. As we only have local information, we use degree of the node in the Lateral Inhibition process.

For Lateral Inhibition, we consider that a node v_i broadcasts and stores a message containing following information: the identity of the head node to which v_i is associated (h_i), its *hopcount* from h_i and the degree of h_i (deg_{h_i}), where $v_i \in V_i$. Initially, all the nodes, $v \in V$, consider themselves as heads, i.e. $H = V$, and store their own information, i.e., $h_i = v$, *hopcount* = 0 and $deg_{h_i} = deg_v$. Each node, $v \in V$, then broadcasts this information to its neighbors, L_v . Similarly, v receives information from each of its neighbors and subsequently updates the information stored in it. Thus, a node replaces its stored values, if the stored degree, deg_{h_i} , is less than that of the received value and *hopcount* + 1 is less than g , where g is the gradient or the desired size of the regions. Further, if the stored and the received deg_{h_i} are same, the node decides to update the stored information based on lower *hopcount* value. If the *hopcount* is also same, then the node randomly decides to update the stored information to received information. The node v then broadcasts the updated information after incrementing the *hopcount* by 1. Subsequently, v removes itself from H , i.e., $H = H - \{v\}$, and inhibits itself from acting as the regional head. The process continues until all the nodes within g hops from the maximum degree node reach a consensus about the head node. Due to g , the algorithm assigns same h_i to all the nodes within g hops of the head node. We call the nodes having same h_i to belong to one region, G_i . The nodes lying at different *hopcount* from the h_i virtually creates a gradient of different hops around h_i , (Cf. Fig. 3(e)). In the end, the algorithm tags a node with no neighborhood as the head as it has remained uninhibited, (Cf. Fig. 3(c)). The regions created differ from other Lateral Inhibition

Notation	Meaning	Notation	Meaning
A	simulation area	g	gradient
G	network with set of vertices V and set of edges E	g_{max}	maximum gradient
G_i	region $G_i G_i \subset G$ with set of vertices V_i and set of edges E_i	e_bet_v	Egocentric Betweenness of v w.r.t. its cluster
N	number of regions formed	$hops(v, w)$	hopcount between node v and w
v	node $ v \in V$	$v_i(x, y)$	virtual coordinates of v in the region G_i
v_i	node v in region $G_i v_i \in V_i$	$v_i(x^*, y^*)$	updated virtual coordinates of v in the region G_i
r	transmission radius	ϵ	error margin
r_b	Bettstetter transmission radius	M	max antenna elements available with v
ρ	average node density	m	number of antenna elements used by v to beamform $ m \in [2, M]$
ID_v	identification number of node v	RC_v	set of centroid nodes reachable from v with their hopcount that are within g_{max} hops from v when v is not beamforming
L_v	neighbor list of $v v \in V$	RC_v^*	set of centroid nodes reachable from v with their hopcount when v is beamforming
$L_{v,i}$	neighbor list of v in the region $G_i v \in V_i$	θ	beam direction, i.e., the sector
ℓ_{min}	minimum number of neighbors used for creating a non-uniform distribution	B_b	boresight direction
deg_v	size of L_v , i.e., degree of v	B_l	beam length
H	set of all region heads	B_w	beam width
h_i	head node of the region $G_i h_i \in H$	APL	Average Path Length
C	set of all centroid nodes	CC	Clustering Coefficient
c_i	centroid node of the region $G_i c_i \in C$	ULA	Uniform Linear Antenna Array
P	set of all peripheral nodes	$GSCC$	Giant Strongly Connected Component
P_i	set of peripheral nodes in the region $G_i P_i \in P$	GIN	Giant In Component
\wp_i	peripheral node $ \wp_i \in P_i$		
\wp_{\wp_i}	peripheral neighbor of $\wp_i \wp_{\wp_i} \in P_i$		
S	Set of nodes neither in C nor in P		

TABLE I
NOTATIONS AND THEIR MEANING.

algorithms, [22], in a way that our algorithm creates regions that are not limited to 1 hop, (Cf. Fig. 3(c) and Fig. 3(d)). However, the Lateral Inhibition technique does not guarantee that the head nodes identified above have a high Closeness Centrality value and are the most central nodes, (Cf. Fig. 2).

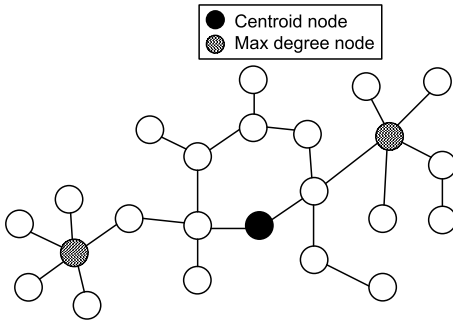


Fig. 2. The max degree nodes are not at the center of the region. The Closeness Centrality of these nodes is less.

We thus now describe the steps for the centroid node identification in a given region, G_i , created using Lateral Inhibition described earlier. Due to the global properties of the Closeness Centrality and unavailability of any *GPS* facilities within the nodes, we take insights from existing algorithms on self-organizing virtual coordinate systems. In self-organizing virtual coordinate system, the nodes identify their own coordinates relative to their neighborhood in the network. We however, make use of self-organizing virtual coordinate system to calculate centroid of the region. Existing techniques on self-organizing virtual coordinate system include [34], [35], [36], [37], [38], [39], [40], [41]. These studies deploy various mechanisms to reach consensus. We use a method for achieving consensus on centroid location based on self-organizing virtual coordinate techniques that rely on averaging of local neighborhood values [38], [40]. This allows us to limit the information required to a single hop, and thereby have minimum communication

overheads.

Thus, in our algorithm, all nodes $v_i \in V_i$ in G_i assign themselves randomly selected virtual xy coordinates, $v_i(x, y)$. The identity of the nodes in the virtual coordinate system, however, remains the same. The nodes then communicate to their neighbors in G_i these coordinates, i.e., $L_{v,i}$. Using the coordinates of their local neighborhood, the nodes compute an average of the coordinates, $v_i(x^*, y^*)$, and broadcast the average coordinates to their neighbors. The neighbors in turn use these coordinates to compute a new average. This process continues until all nodes in the region reach consensus of having same average xy coordinates of the centroid.

The self-organizing virtual coordinate technique reveals the location of the centroid node in the self-organizing virtual coordinate system but not the identity of the node that is to be termed as centroid. In order to identify the centroid node of the region, nodes use their initially assigned virtual coordinates and the newly found average xy coordinates. Each node v_i checks if $v_i(x, y) = v_i(x^*, y^*) \pm \epsilon$, where ϵ is the error margin, and declares itself as the centroid. This process might result into multiple nodes declaring themselves as the centroid as two or more nodes can lie within the ϵ range of $v_i(x^*, y^*)$. To avoid this, a node also considers its Degree and Egocentric Betweenness². The nodes within ϵ range of $v_i(x^*, y^*)$ share this information among themselves. Subsequently, the node having maximum sum of Degree and Egocentric Betweenness declares itself as the centroid of the region. As the node has same identity in the self-organizing virtual coordinate system as in the real coordinate system, the centroid node in the self-organizing virtual coordinate system will also be the centroid in the real coordinate system. After the identification of the centroid nodes, the centroid nodes broadcast their information in the network. All nodes then update their stored head information to their respective c_i 's and the hopcount to $hops(v_i, c_i)$.

This broadcasting of the centroid node information enables the nodes to build RC_v for future use. RC_v is the set of centroid nodes within g_{max} hops of the node v , where $g_{max} > g$.

²Egocentric Betweenness approximates the Socio-Centric Betweenness very well in the absence of global knowledge [42]

Algorithm 1 represents the algorithmic description of the region formation and the centroid identification process. The Fig. 3(f) shows the centroid nodes for the regions identified in the Fig. 3(c).

2) *Beamforming*: In this part, we describe the steps involved in beamforming. According to the results of [13], it requires only a small fraction of nodes with long link capabilities to achieve small world properties. In a self-organizing environment where all nodes possess beamforming capabilities, it is essential to identify nodes that create long-range beams along with the direction and the width of the beam. Flocking provides us with valuable insights in determining the answers to these questions. We use insights from the Alignment rule of Flocking to identify the set P . Alignment in Flocking is the change in the direction of the node to match its neighbors, in other words the change in the orientation of the node. Further, Alignment rule is, the node has to decide to change the direction and has to find the new direction. We modify the Alignment rule and say that our Alignment rule is only limited to the decision of whether to create the beam or not. The Alignment rule we apply is, thus, to identify the set of peripheral nodes, P_i in the region G_i . Our algorithm uses the *hopcount* of the neighborhood nodes to decide whether or not the node is a peripheral node, φ_i , of the region G_i . If all $L_{v,i}$ of the node v_i have *hopcount* less than or equal to the node's *hopcount* to the c_i , then the node declares itself as a peripheral node. i.e., for a given region G_i with centroid c_i , $\varphi_i \in P_i \iff \text{hops}(\varphi_i, c_i) \geq \text{hops}(L_{\varphi_i}, c_i)$. This implies that, a single unconnected node will become a peripheral node because it does not have any neighborhood. Further, we can also infer that two peripheral nodes can be neighbors of each other due to the equality in the condition.

The peripheral nodes randomly choose the number of antenna elements, $m \in [2, M]$, and use the above rules to beamform. Considering B_l to be equal to $m*r$ in a Sector model, by keeping constant power as used for omnidirectional beam, we can easily compute B_w from eq. (1) as $B_w = \frac{2\pi}{m^2}$. From this we infer that, to cover all the directions, minimum number of sectors that we need to consider is m^2 . The dependency of B_l and B_w on m affects the connectivity of the network. The Fig. 5(a) shows the variation in B_l and B_w when $m > 1$. When B_l is smaller, i.e., when we use less number of antenna elements, the probability of connecting to the neighbors is high as the beam is wider, (Cf. Fig. 5(b)). However, when B_l is longer, i.e., when we use more antenna elements, the probability of connecting to a neighbor is low as the beam is narrower, (Cf. Fig. 5(c)).

As the number of sectors increase exponentially with an increase in the number of antenna elements, there is an increase in the time taken to decide the best sector. Checking all the sectors formed for all $m \in [2, M]$ requires a test of $\frac{(M)(M+1)(2M+1)}{6} - 1$ sectors. The complexity of such a test is $O(M^3)$. This results into more energy consumption at the node. To reduce this energy consumption and the complexity to $O(M^2)$, our algorithm randomly selects the number of antenna elements, $m \in [2, M]$, and only tests the corresponding set of m^2 sectors.

Non-uniformity reduces the size of the giant component in the wireless ad hoc network. It is thus important for the nodes to find different network components and connect them using beamforming. Separation rule of Flocking provides us insight towards this problem. Separation rule states that the nodes should maintain certain distance with their neighbors. Our algorithm applies similar analogy to address the connectivity issue. We say, in order to increase connectivity, nodes create beam in different directions from their peripheral neighbors. Consider $\varrho_{\varphi_i} \in P_i$ as a peripheral neighbor of φ_i then for all ϱ_{φ_i} 's, $\varphi_i(B_b) \neq \varrho_{\varphi_i}(B_b)$ must hold. Here B_b is the boresight direction. To make this decision, if ϱ_{φ_i} of a φ_i decides to create the beam in certain direction, ϱ_{φ_i} informs φ_i about the chosen direction before it actually creates the beam. φ_i then tries to create the beam in another direction. Further, φ_i gives preference

Algorithm 1 Region formation and centroid finding

```

1: Let  $U = uninhibited$ ;
2: Let  $I = inhibited$ ;
3: Let  $ID = identity\ of\ node$ ;
4:  $\backslash\backslash$  Region formation;
5: for all  $v \in V$  do
6:   set  $v_{Status} = U$ 
7:   set  $v_{coordinates} = v_i(x, y)$ 
8:   Initially broadcast( $ID_v, hopcount = 0, deg_v$ )
9: end for
10: repeat
11:    $recv = receive(ID, hopcount + 1, degree)$ 
12:   if  $deg_v < degree \ \& \ hopcount < g$  then
13:      $v_{Status} = I \ \& \ broadcast(recv)$ 
14:   end if
15: until converges
16:  $\backslash\backslash$  Centroid finding;
17: for all  $v_i \in V_i \in V$  do
18:    $v_i(x^*, y^*) = Cent\_finding(v_i(x, y), L_{v,i}(x, y))$ 
19: end for
20: for all  $v_i \in V_i \in V | v_i(x, y) - \varepsilon < v_i(x^*, y^*) < v_i(x, y) + \varepsilon$  do
21:   compute  $sum_{v_i} = sum(deg_{v_i}, e\_bet_{v_i})$ 
22: end for
23: for all  $v_i \in V_i \in V$  do
24:    $c_i = v_i | v_i = max\{sum_{v_i}\}$ 
25:    $C = C + v_i$ 
26: end for
27: for all  $v \in V$  do
28:   formulate  $RC_v$ 
29: end for

```

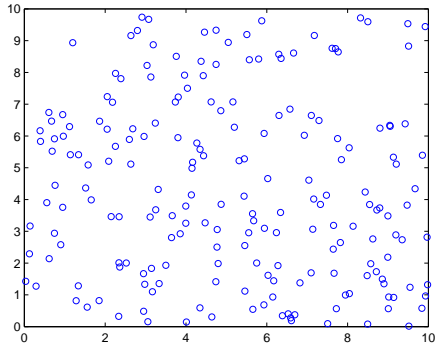
to connect to the nodes in other region rather than that of its own. This increases the possibility of connecting to an isolated region. The Fig. 4 shows two node w and x which were initially neighbors of each other, create beams in different direction in order to increase connectivity.

Nevertheless, we still have to address the best direction of the beam and the knowledge of whether a φ_i has a node within its 1 hop. We address these problems next in this section.

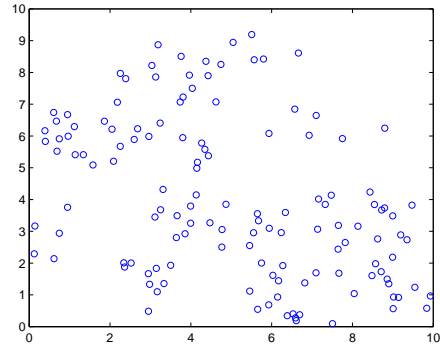
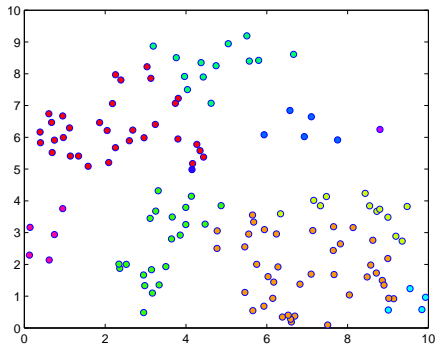
To the above-mentioned problem, we use analogy of Cohesion rule of Flocking to determine the best direction of the beam. In Flocking, Cohesion rule states that a node should move towards the centroid of the neighborhood to remain connected to all of its neighbors. We apply this definition of Cohesion in our algorithm because we want to bind a peripheral node with other nodes in minimum hops. From the previous section, we already know that the centroid node has the highest Closeness Centrality value in a given region. Directing the peripheral node's beam towards the centroid node would help reduce the average distance of the peripheral node to other nodes of the region in which the centroid node lies.

Combining Separation and Cohesion rules as discussed above, we can say that, if the centroid node chosen by the peripheral node and the peripheral node itself were not connected initially, connecting them would help in increasing the connectivity, (Cf. Fig. 4). On the other hand, if the centroid node chosen by the peripheral node was within some hops from the peripheral node, it will lead to the reduction in the *APL*.

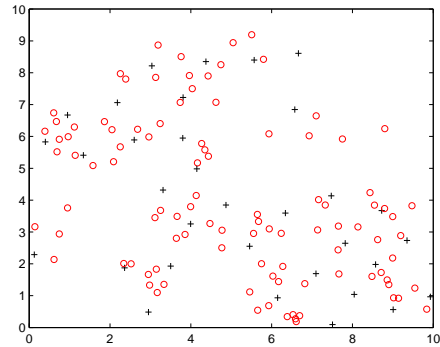
To account for choosing the correct centroid to connect, the peripheral node, φ_i , builds $RC_{\varphi_i}^*$, a set of all centroid nodes



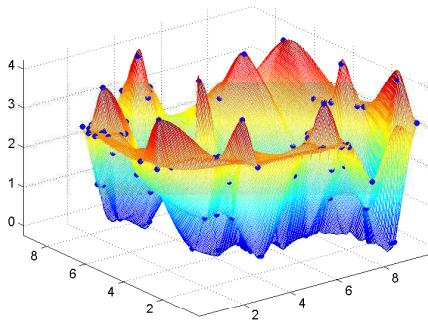
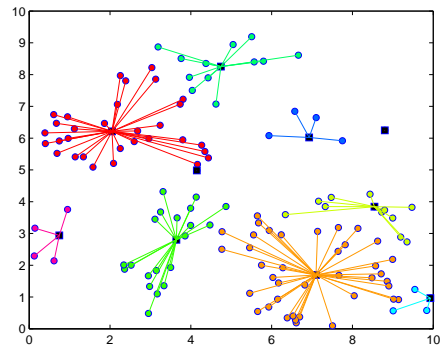
(a) Uniform Node Distribution.

(b) Distribution after applying Thinning process with $r_b = 1$ and $\ell_{min} = 5$.

(c) Identified regions in the deployment shown by the Fig. 3(b).



(d) Identified uninhibited nodes created using the [22] algorithm for the deployment shown by the Fig. 3(b). As there is only one head in the region, the number of uninhibited nodes directly refers to the number of regions created. The nodes shown with + are the uninhibited nodes while the nodes shown with o are the inhibited nodes.

(e) The gradient of the nodes created using the *hopcount* for the regions created in the Fig. 3(b). The peaks show the centroid nodes while the valley show nodes with the max gradient value.

(f) Association of the nodes to the centroid nodes. The centroid of the region is marked with a black square.

Fig. 3. Region Formation and Centroid identification using $g < 5$.

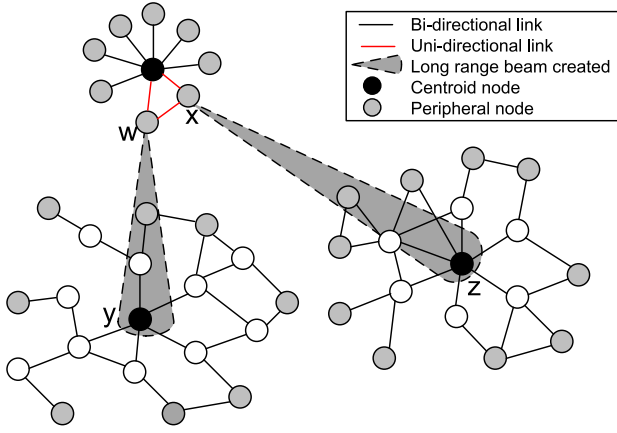
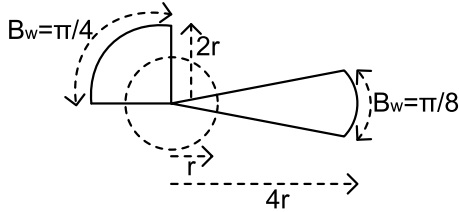
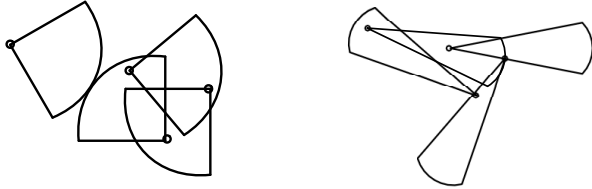


Fig. 4. Nodes beamform in different directions. Two peripheral nodes w and x which were initially neighbors of each other, create beams in different directions. In order to have increased connectivity, the node w creates a beam towards the region containing the centroid node y , while the node x creates a beam towards the region containing the centroid node z . The maximum gradient value for Lateral Inhibition is 4.



(a) The difference in the beam properties when a φ_i uses different number of antenna elements.



(b) Connectivity when 2 antenna elements are used.

(c) Connectivity when 4 antenna elements are used.

Fig. 5. Relationship between beam properties and connectivity.

reachable when it is beamforming. To determine $RC_{\varphi_i}^*$, the peripheral nodes sweep through all the sectors (m^2) created with the chosen number of antenna elements except the sectors in which φ_i 's have created the beam. If $RC_{\varphi_i}^* - RC_{\varphi_i} \neq \emptyset$ and $|RC_{\varphi_i}^* - RC_{\varphi_i}| > 1$, i.e., φ_i identified two or more potential centroid nodes, assuming the *hopcount* to these centroid nodes as ∞ the decision to connect to one of them is randomly made. However, if $RC_{\varphi_i}^* - RC_{\varphi_i} = \emptyset$, i.e., no new centroid is found, the φ_i decides to connect to farthest centroid node in RC_{φ_i} . As we know that *APL* is dependent on $\sum_{v,w \in V, v \neq w} hops(v,w)$ any reduction in this summation will lead to a reduced network path length. In order to have maximum reduction in the path length, the node should connect to the farthest centroid. If the farthest centroid node was the c_i , then φ_i beamforms towards it. However, this decision also depends on the *hopcount* between c_i and φ_i . Creating the beam toward the centroid that is less than two hops away will only reduce the initial neighborhood but not the *APL*. In this case φ_i drops the decision of being the peripheral node and remains omnidirectional. The Fig. 6(a) and

the Fig. 6(b) depicts the same. In the Fig. 6(a), node x is 5 hops away from y while it is 4 hops away from z and 2 hops away from the centroid of the region in which x lies. Thus, in order to have a reduced path length, node x decides to create beam towards y . On the contrary, in the case when the node x does not have the previously stored information about the centroid nodes y and z , the node considers *hopcount* to these centroid nodes as ∞ and randomly chooses one of them to connect to, (Cf. Fig. 6(b)).

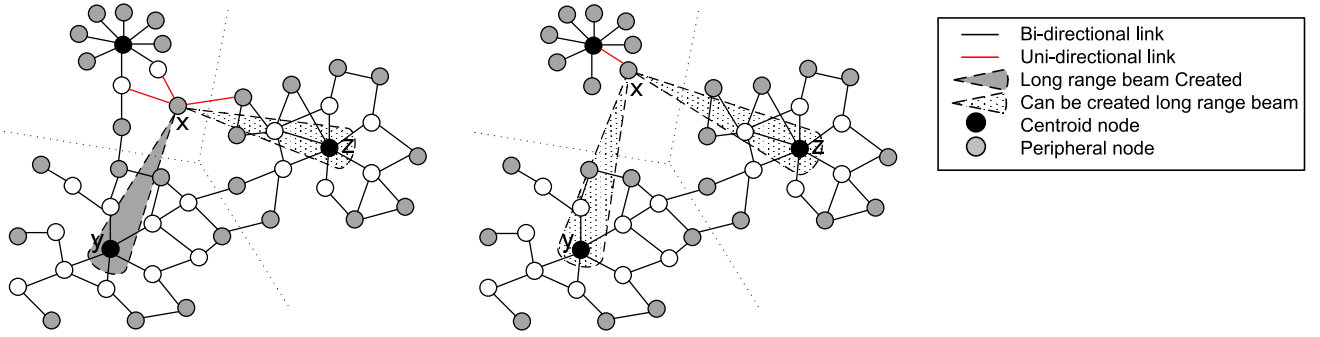
Whenever a peripheral node creates a beam towards a centroid node that is more than 1 hop away, asymmetric link may arise. This is due to the fact that the B_l of peripheral node is $m * r$ while B_l of a centroid node is r , in other words, $\frac{B_l \text{ of Centroid}}{B_l \text{ of peripheral}} = \frac{1}{m}$. Due to this difference, peripheral nodes will not know if they got connected to the centroid of other region or not. We propose to solve this issue as, when a centroid node receives information about the node trying to connect to it, it just for one time instant, to acknowledge the reception, creates the beam back to the node. We do this after determining angle of incidence of the beam. This works well for both connected and unconnected components. Algorithm 2 represents a brief algorithmic description of beamforming using Flocking rule analogy. The Fig. 7 shows the new network created after running our algorithm on the network shown in the Fig. 3(b).

Algorithm 2 Beamforming using Flocking Analogy

```

1: \ \ Alignment;
2: for all  $v_i \in V_i \in V$  do
3:   if  $hops(v_i, c_i) > hops(L_{v,i}, c_i)$  then
4:      $P_i = P_i + \{v_i\}$ 
5:      $P = P + \{v_i\}$ 
6:   end if
7: end for
8: \ \ Separation;
9: for all  $\varphi_i \in P_i \in P$  do
10:  set  $m$ 
11:  for all  $m^2$  Sectors  $|_{\varphi_i}(B_b) \notin \text{Sectors}$  do
12:     $RC_{\varphi_i}^* = RC_{\varphi_i}^* + \{\text{reachable centroid nodes}\}$ 
13:  end for
14: end for
15: \ \ Cohesion;
16: for all  $\varphi_i \in P_i \in P$  do
17:  if  $RC_{\varphi_i}^* - RC_{\varphi_i} \neq \emptyset$  then
18:    for all  $c \in RC_{\varphi_i}^* - RC_{\varphi_i}$  do
19:       $h = h + hops(\varphi_i, c)$ 
20:    end for
21:  else
22:    if  $RC_{\varphi_i} \neq \emptyset$  then
23:      for all  $c \in RC_{\varphi_i}$  do
24:         $h = h + hops(\varphi_i, c)$ 
25:      end for
26:    else
27:       $P_i = P_i - \{\varphi_i\}$ 
28:    end if
29:  end if
30:   $beamtonode = \max\{h\}$ 
31:   $\theta = \text{Sector containing beamtonode}$ 
32: end for

```



(a) One component with three regions when $g = 3$. Here, the node x can create the beam towards y or z , but because the *hopcount* to y is more than z , node x creates the beam towards y .

(b) Three unconnected components with three regions when $g = 3$. Here, the node x can create the beam either towards y or z , but because the *hopcount* to y and z is same as ∞ , x randomly decides between y and z to connect to.

Fig. 6. Beamforming priority.

III. FORMAL DEFINITIONS

Definition 1. Assume a centroid c_i of the region G_i , and a node v_c in V_i which has the highest Closeness Centrality, then

$$\begin{aligned} \text{Closeness}(v_c) &= \arg \max_{\forall v_i \in V_i} [\text{Closeness}(v_i)] \\ \text{Closeness}(c_i) &\simeq \text{Closeness}(v_c) \end{aligned} \quad (2)$$

Definition 2. The node v_i with neighborhood $L_{v,i}$ of the region G_i with centroid c_i is a peripheral node $\iff \text{hops}(v_i, c_i) \geq \text{hops}(L_{v,i}, c_i)$.

Lemma 1. The expected number of nodes remaining after applying the thinning processes, [24], on a uniformly distributed network is

$$E(n) = \rho A \left(1 - \frac{\Gamma(r_b, \rho r_b^2 \pi)}{(r_b - 1)!} \right) \quad (3)$$

where $E(n)$ is the expected number of nodes remaining after the thinning process is applied, ρ is the initial node density in a given area A and $\Gamma(r_b, \rho r_b^2 \pi)$ is the incomplete gamma function.

Lemma 2. The separation between any two head nodes is between $(g, 2g + 1]$ where g is the hopcount used to create the region, [21].

Proof: Consider a head node with a gradient g around itself. All the nodes within g hops from the head node will be in its region. A node which is more than g hops away will lie in another region. If in the neighboring region, a head node does not have any gradient around it, then the distance between the two head nodes in hops will be $g + 1$. On the other hand, if the neighboring region also has a gradient g around it, then the distance between two head nodes in hops will be $2g + 1$. ■

Lemma 3. The number of regions is equal to number of centroid nodes and each region has exactly one centroid node.

Proof: Our algorithm computes the centroid of the region based on average of coordinates, Degree and Egocentric Betweenness of the node for each region. According to our algorithm, the nodes are termed as centroid if the node falls within ε range of the centroid coordinate estimation algorithm and have maximum sum of Degree and Egocentric Betweenness. If still there are multiple nodes that are termed as centroid nodes, the nodes randomly decide for being the centroid and thus only one node is chosen as centroid. The value of ε is thus an important factor in the estimation of the centroid node. Also, smaller ε will tend to provide better estimation of the centroid nodes. As there is only one centroid node per region, the number of centroid nodes is equal to the number of regions. ■

Lemma 4. If a node is not a centroid node, it is connected to a centroid node.

Proof: Our algorithm identifies regions and their centroid nodes. An identified region is always connected, i.e., all the nodes in the identified region are connected to each other. Further, there is one and only one centroid node in a region, ref. lemma 3. Thus for a given region, all nodes that are not centroid are connected to the centroid node. ■

Lemma 5. An unconnected node is both the centroid node as well as the peripheral node.

Proof: A single unconnected node does not have any neighborhood. It thus remains uninhibited at the end of the region formation phase and becomes the head. As it is lacking any neighborhood, the node does not have any gradient around itself and is the only node in the region. In this region, the average coordinates perfectly match the virtual coordinates of the node. Thus requiring no further computation to correctly identify the centroid node.

This node is also the peripheral node as the condition of Definition 2 holds true because of the unavailability of the neighborhood. ■

Lemma 6. For a node distribution and fully connected network with average node density ρ and total number of nodes $|V|$, then $|C|$ is bounded by $\frac{|V|}{\rho g^2 r^2 \pi}$ and $\frac{|V|}{\rho g^2 r^2 \sqrt{3}}$.

Proof: From lemma 2, the hop distance between two heads is bounded by $(g, 2g + 1]$.

Case 1 (Lower Bound): When the heads are separated by $2g + 1$ hops, the number of regions formed are less. The number of nodes in one region is $\rho g^2 r^2 \pi$. Thus, the total number of nodes in all the N regions is $|N| \rho g^2 r^2 \pi$. As the total number of nodes are $|V|$, $\therefore |N| = \frac{|V|}{\rho g^2 r^2 \pi}$. From lemma 3 $|C| = |N|$, $\therefore |C| = \frac{|V|}{\rho g^2 r^2 \pi}$.

Case 2 (Upper Bound): When all the heads are separated by $g + 1$ hops, the number of regions formed are more. A head in such a case is connected to only 6 other heads. This can be visualized as a hexagon with vertex-vertex distance equal to $g + 1$ and a node at the center of hexagon. Each of the vertex nodes are shared between 3 other hexagons. Thus, the total number of heads that are exclusive for the hexagon are $\frac{6}{3} + 1 = 3$. In other words, there are 3 heads in an area of $\frac{6g^2 r^2 \sqrt{3}}{2}$. Thus, for the area $= \frac{|V|}{\rho}$, $|C| = \frac{|V|}{\rho g^2 r^2 \sqrt{3}}$. ■

Lemma 7. Consider a network with j components ($j > 1$), average density of the nodes as ρ_k and number of nodes as $|V_k^j|$ for $k \in j$, $|C|$ is bounded by $\sum_{k=1}^j \frac{|V_k^j|}{\rho_k g^2 r^2 \pi}$ and $|V|$, where $|V| = \sum_{k=1}^j |V_k^j|$.

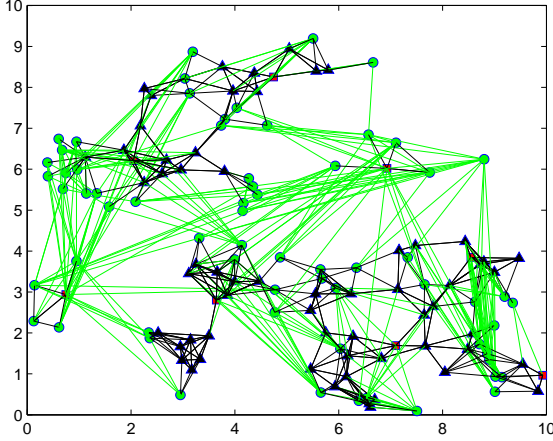


Fig. 7. Nodes beamforming towards other region's centroid created for the Fig. 3(b) using $g < 5$. The nodes marked in green beamform. The directional beams are also shown in green. The nodes marked with black triangle do not beamform. The nodes marked with red square are the centroid nodes.

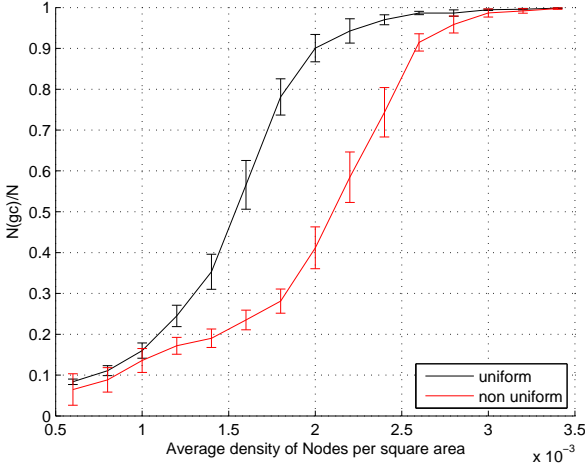


Fig. 8. Percolation of the giant component for nodes distributed uniformly and non-uniformly. We use $r_b = 30m$ and $\ell_{min} = 5$ to achieve non-uniform distribution of nodes. There is a difference in the values of the size of the giant component at the same average density because the algorithm used to generate non-uniformity [24] tends to create clusters of nodes that might be unconnected. This leads to a network that is less connected than the uniformly deployed network. However, when the density increases the size of the clusters also increases.

Proof: From lemma 2, the hop distance between two heads is bounded by $(g, 2g + 1]$.

Case 1 (Lower Bound): Consider k^{th} component of the network. When the heads are separated by $2g + 1$ hops, the number of regions formed is less. The number of nodes in one region is $\rho_k g^2 r^2 \pi$. Thus, the total number of nodes in all the regions in the component is $N_k \rho_k g^2 r^2 \pi$, where N_k are the number of region in k^{th} component. But as the total number of nodes were assumed to be $|V_k^j|$, $\therefore N_k = \frac{|V_k^j|}{\rho_k g^2 r^2 \pi}$. Thus for all the components, the number of regions formed is $|N| = \sum_{k=1}^j N_i = \sum_{k=1}^j \frac{|V_k^j|}{\rho_k g^2 r^2 \pi}$. From lemma 3, $|C| = |N|$, $\therefore |C| = \sum_{k=1}^j \frac{|V_k^j|}{\rho_k g^2 r^2 \pi}$

Case 2 (Upper Bound): Upper bound to the number of regions arises when all nodes in the network are disconnected. Thus, all

nodes in such a case will be uninhibited thereby becoming region heads. Thus $|C| = |V|$. ■

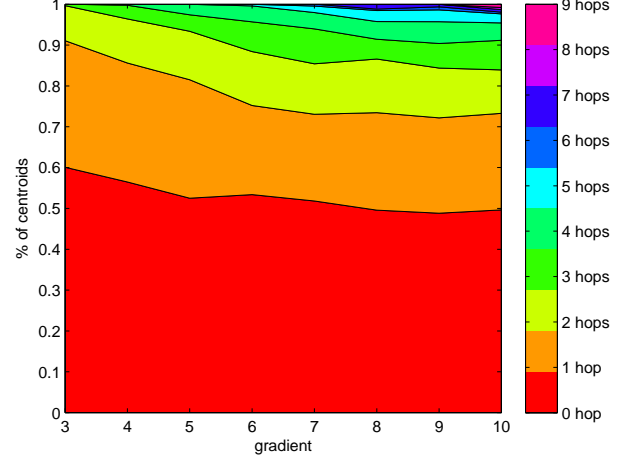


Fig. 9. Relationship between centroid nodes and the nodes having maximum Socio-Centric Betweenness.

Lemma 8. For a node distribution and fully connected network, and using lemma 6, the number of peripheral nodes in the network is bounded by $\frac{|V|(2g+1)}{g^2}$ and $\frac{|V|(2g+1)\pi}{g^2\sqrt{3}}$.

Proof: Peripheral nodes are the nodes lying in the outer most gradient of the region. Thus, the number of nodes in the g^{th} gradient of a region $= \rho g^2 r^2 \pi - \rho(g-1)^2 r^2 \pi = \rho(2g+1)r^2 \pi$

Now using lemma 6, the number of peripheral nodes for all regions thus varies between $\frac{|V|(2g+1)}{g^2}$ and $\frac{|V|(2g+1)\pi}{g^2\sqrt{3}}$. ■

Lemma 9. For a node distribution and network with j components ($j > 1$), and using lemma 7 and lemma 5, the number of peripheral nodes in the network is bounded by $\sum_{k=1}^j \frac{|V_k^j|(2g+1)}{g^2}$ and $|V|$.

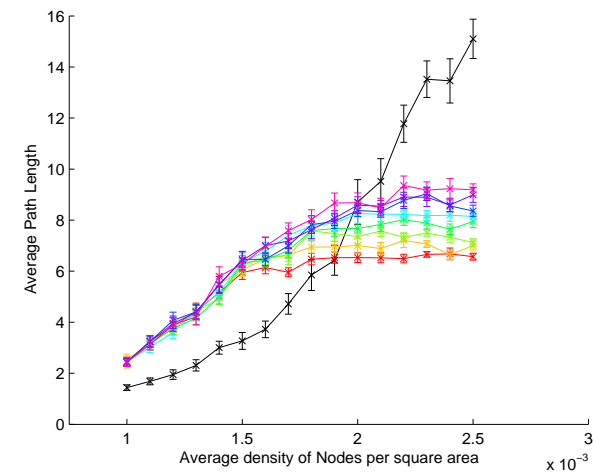
Proof: Peripheral nodes are the nodes lying in the outer most gradient of the region. Thus, the number of nodes in g^{th} gradient of a region in k^{th} component $= \rho_k g^2 r^2 \pi - \rho_k(g-1)^2 r^2 \pi = \rho_k(2g+1)r^2 \pi$.

Now using lemma 7 and lemma 5, the number of peripheral nodes for all regions thus varies between $\sum_{k=1}^j \frac{|V_k^j|(2g+1)}{g^2}$ and $|V|$. ■

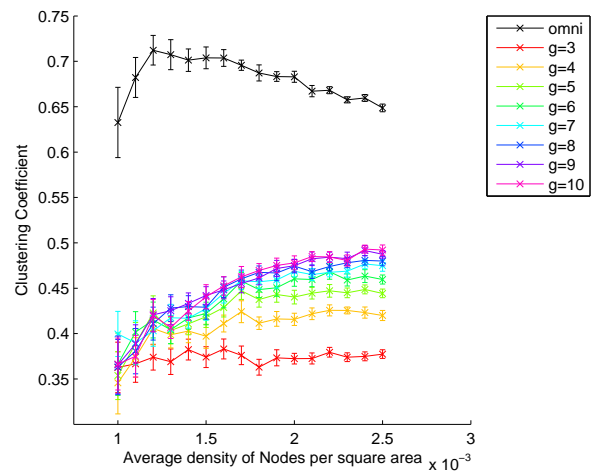
IV. SIMULATION SETUP

We use a simulation area of $A = 500m \times 500m$ to simulate our algorithm. r_b and ℓ_{min} are set to $30m$ and 5 respectively to achieve the non-uniform distribution of node throughout the simulation area. The non-uniform node distribution enables us to visualize the real world scenarios. The range of average density, ρ , of nodes per unit area is set to $[1 \times 10^{-3}, 2.5 \times 10^{-3}]$. We make the choice of this range for ρ after considering the percolation of the giant component for the non-uniform node deployment, (Cf. Fig. 8). Initially, each node operates in omnidirectional mode using $m = 1$ antenna element with the omnidirectional radius as $r = 30m$. We set the maximum number of antenna elements that the nodes are equipped with to $M = 6$. The separation between two antenna elements computed using *WiFi* frequency, $f = 2.4GHz$. Through our simulations, we explore the effect on connectivity, *APL* and *CC* by varying the node densities and the gradient.

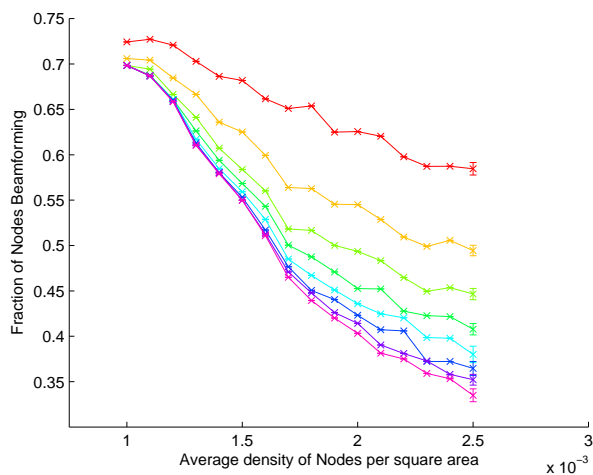
We use *MATLAB* to simulate our algorithm with a confidence interval of 95%. We average All the results over 50 topologies.



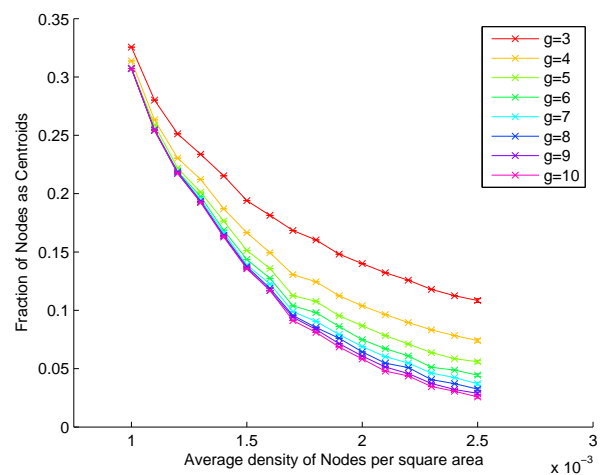
(a) Average path length in hops.



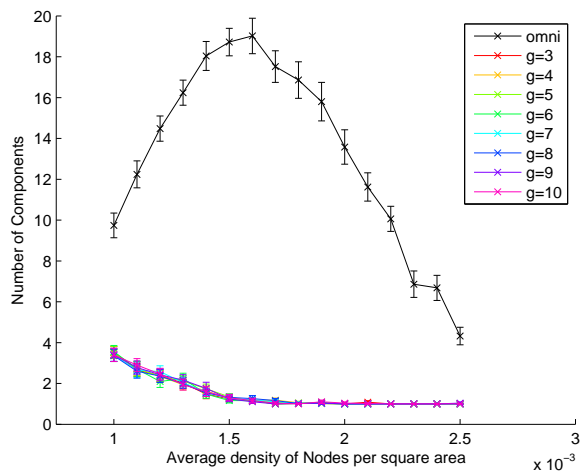
(b) Clustering Coefficient.



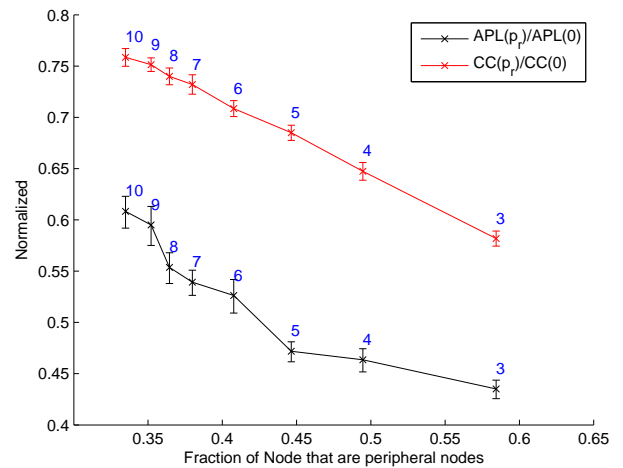
(c) Fraction of nodes designated as Peripheral nodes.

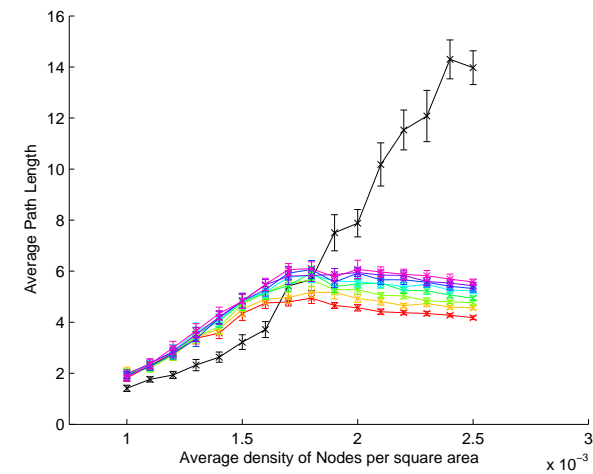


(d) Fraction of nodes designated as centroid nodes.

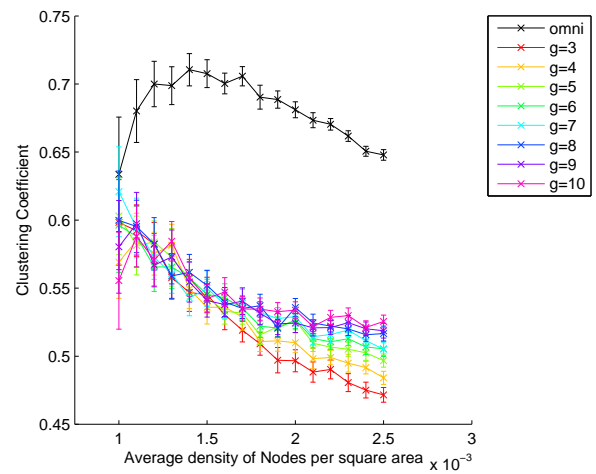


(e) Number of components in the network.

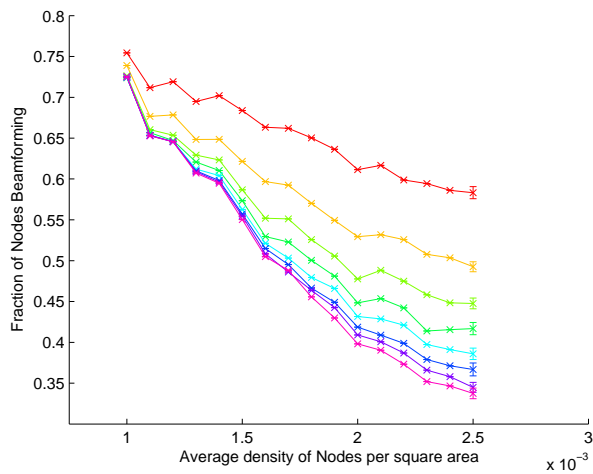
(f) Normalized directional APL and CC for $N = 625$ showing the effects of the gradient.Fig. 10. Results obtained for $g \in [3, 10]$, when we use Sector model and non-uniform node distribution.



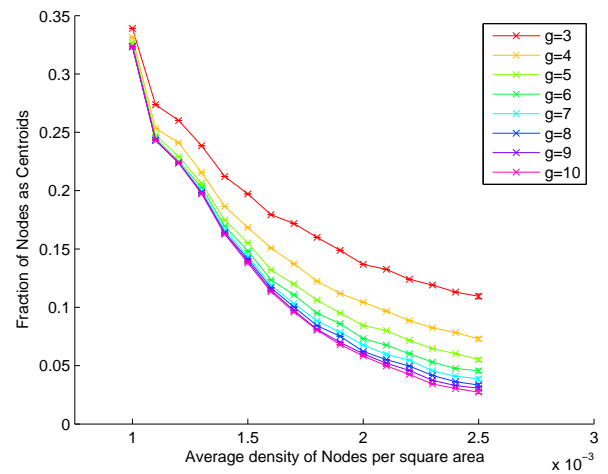
(a) Average path length in hops.



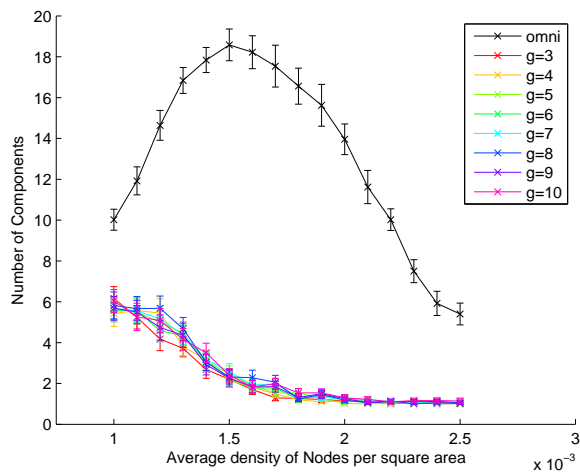
(b) Clustering Coefficient.



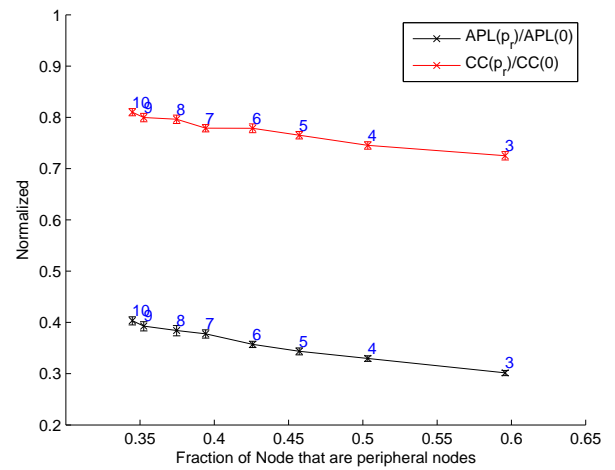
(c) Fraction of nodes designated as Peripheral nodes.



(d) Fraction of nodes designated as centroid nodes.



(e) Number of components in the network.

(f) Normalized directional APL and CC for $N = 625$ showing the effects of the gradient.Fig. 11. Results obtained for different $g \in [3, 10]$, using ULA model and non-uniform node distribution.

V. RESULTS AND ANALYSIS

First, we prove the correctness of the centroid finding in the region. For this, we compute the relation between the nodes that have maximum Socio-Centric Betweenness and the centroid nodes in the region. If the centroid node has the highest Socio-Centric Betweenness in the region, then the algorithm found centroid node correctly, (Cf. Fig. 9). This depends on the value of the gradient. Larger gradients decrease the Socio-Centric Betweenness rank of the centroid node in the region. As the gradient increases, more nodes are now associated to a region thereby increasing the possibility of occurrences of the bridge nodes (bridge nodes have high Socio-Centric Betweenness value). Thus, we also calculate the distance in hops between the centroid node and the maximum Socio-Centric Betweenness node. According to the results, (Cf. Fig. 9), for a g , the percentage of centroid nodes that also have high Socio-Centric Betweenness is more and all the centroid nodes in the network are within $hopcount < g$. The Fig. 9 however shows that for any $g \in [3, 10]$ more than 95% of the time the centroid node is within 4 hop distance to the maximum Socio-Centric Betweenness value node and it is within 1 hop 60% of the time.

Further, we use $g \in [3, 10]$ to obtain the results when the Sector model is used in a non-uniformly distributed network, (Cf. Fig. 10). The Fig. 10(a) shows the effect of beamforming on the APL . The APL obtained in omnidirectional case is initially less than that obtained for the directional cases because the density of the nodes in the component is low. When the algorithm induces directional beams, due to the inclusion of the nodes in other network components, there is an increase in the APL . The APL for the directional case is less than that of the omnidirectional case when $\rho > 2 * 10^{-3}$ due to the fact that the nodes connect to the centroid node of other regions in the different component as well as in the same component. The gradient affects the APL . The lower the value of the gradient is, higher is the number of nodes that beamform, (Cf. Fig. 10(c)), leading to more shortcuts and in turn more reduction in the APL . For $\rho = 2.5 * 10^{-3}$ and $g = 10$, there is a reduction of almost 40% in the APL while there is a reduction of almost 55% for $g = 3$, (Cf. Fig. 10(f)). However, for $\rho = 1 * 10^{-3}$ and $g \in [3, 10]$ when most nodes are unconnected, there is an increase of 70% in APL due to the above-mentioned facts.

The introduction of the long-range beams also causes the CC to change, (Cf. Fig. 10(b)). For very low-density networks, the CC for the directional case is less because beamforming leads to loss in the initial neighborhood. However, for higher density networks, the CC does not vary as much as the APL (Cf. Fig. 10(f)). For $\rho = 2.5 * 10^{-3}$, there is a reduction of 25% and 38% for $g = 10$ and $g = 3$ respectively. However, for $\rho = 1 * 10^{-3}$ and any $g \in [3, 10]$, the reduction in CC is almost 40%. The CC for directional case for $g < 6$ and $\rho \in [1 * 10^{-3}, 2.5 * 10^{-3}]$ is almost constant. This implies that the directional network shows modularity where CC is independent of $|V|$ and evolves towards hierarchical network [43]. However, when $g \in (6, 10]$ the evolution towards hierarchical networks cannot be justified.

The number of components in the network can define connectivity. In a very low-density omnidirectional network, the number of disconnected components is higher, (Cf. Fig. 10(e)). The number of disconnected components increases to a certain maximum and then decreases as the density increases. This is because, for a high density, all nodes can find at least one neighborhood node within their reach. In addition, as the number of components decreases, the connectivity increases. For the directional case however, as nodes beamform towards different components with the objective of increasing connectivity, the number of disconnected components is less than that of the omnidirectional case.

The size of the giant component can also explain the connectivity of the network. For the directed graphs however, [44] defined the giant component using the Giant Strongly Connected

Component ($GSCC$)³ and the Giant In-Component (GIN)⁴. Thus, we calculate the size of $GSCC$ and GIN . We further show the difference between the size of the giant component for omnidirectional network, $GSCC$ and GIN . As stated in [44] that $GSCC \subset GIN$, we also observe that GIN is a bigger set and contains more nodes than $GSCC$. GIN reaches percolation very early, (Cf. Fig. 12). Comparing the size of the $GSCC$ of directional network with the giant component of the omnidirectional network, (Cf. Fig. 8), we see that the size of $GSCC$ varies between $[0.84, 0.94]$ for $\rho = 2 * 10^{-3}$ for different values of the gradient while the size of giant component for the omnidirectional network is 0.41. Thus, we observe an increase of almost 2.1 times. The Fig. 13 shows an increase of almost 2.2 times when we compare of size of the $GSCC$ and the GIN for $g = 6$ with the giant component of the omnidirectional network.

The number of centroid nodes ($|C|$) depends on the value of the gradient, (Cf. Fig. 10(d)). For a low-density network, the value of the gradient does not matter while as the density increases the value of the gradient affects the number of regions formed. As the gradient increases, more nodes inhibit leading to less number of regions. The difference between the number of regions formed for $g = 3$ and $g = 10$ is of 40 for $\rho = 2.5 * 10^{-3}$ while the difference for $\rho = 1 * 10^{-3}$ is very less.

The value of the gradient used also affects the number of peripheral nodes ($|P|$) identified, (Cf. Fig. 10(c)). For a low gradient value, as there are more regions, more nodes are included in P because of the reduced neighborhood with respect to the region. However, when the value of the gradient is more, $|P|$ is less because there are more nodes in the region and the nodes have relatively more neighbors to check before making the decision of beamforming. $|P|$ greatly affects the number of unidirectional paths. However, it has an adverse effect on the CC . As the number of peripheral nodes increases, unidirectional paths between the nodes also increases leading to more loss in the CC . For $\rho = 1 * 10^{-3}$ and $g \in [3, 10]$, the difference between the number of peripheral nodes is almost negligible. For $\rho = 2.5 * 10^{-3}$, however, the number of peripheral nodes varies by more than 120 as the regions formed for lower gradient are more.

Our algorithm affects the APL and the CC of the network when we use ULA model, (Cf. Fig. 11). On the other hand, it does not affect $|P|$ and $|C|$. No dependency of the ULA model on $|P|$ and $|C|$ is rightly justified because these sets are built when the network was omnidirectional, (Cf. Fig. 11(c), 11(d)). However, there is a reduction of almost 60% and 68% in the APL for higher gradient value and for low gradient value respectively. On the other hand, there is no considerable reduction in the CC . The reduction in the CC is only between 19% to 22%. Due to variation in B_w for different B_b in ULA model (Cf. Fig. 16), the values obtained for the APL , the CC and connectivity are different from that of the Sector model. From the Fig. 14 we observe that, for higher density networks, the change in the APL for the ULA model is more than that of the Sector model while the CC changes at a much lower rate.

Until now, we have shown that small world properties are achieved and connectivity be increased in a non-uniformly deployed network. However, it is also important to show the complexity of the algorithm. Due to the storage of three required data values in the region formation phase, neighborhood information and the knowledge about being the peripheral node for both itself and its neighbors is needed. Thus the required memory size is of the order $O(3(d+r)+d+1)$ where d is the size of the neighborhood and r is the size of reachable centroid nodes. For high-density network, reaching consensus in the region formation and the centroid finding phase is time consuming.

³ $GSCC$ in a directed graph is the length of the largest cycle in the graph component.

⁴ GIN is the set of nodes in the component which can connect to $GSCC$.

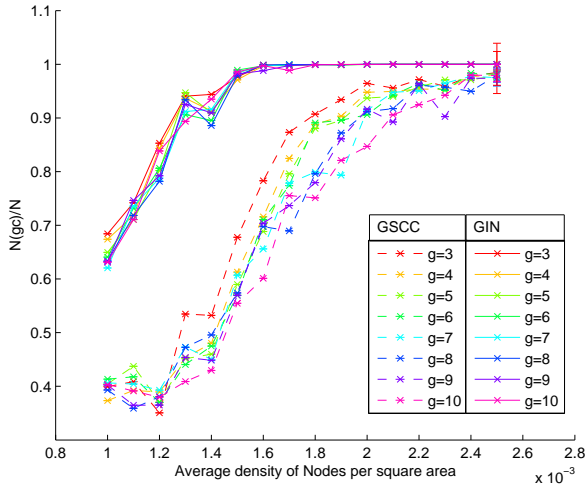


Fig. 12. Variation in the size of the *GSCC* and the *GIN* for different density of nodes and $g \in [3, 10]$.

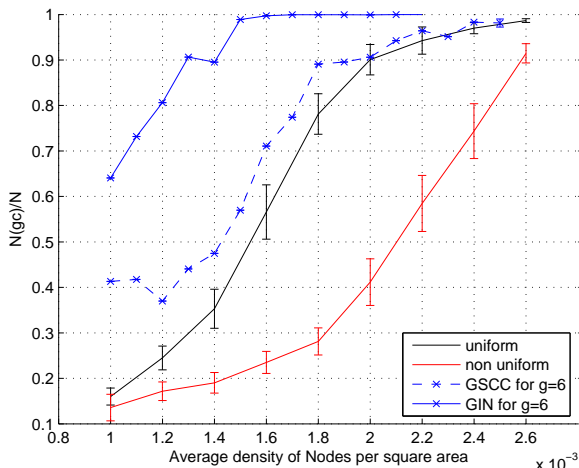


Fig. 13. Comparison of size of the *GSCC* and the *GIN* for directed network with that of omnidirectional network for $g = 6$.

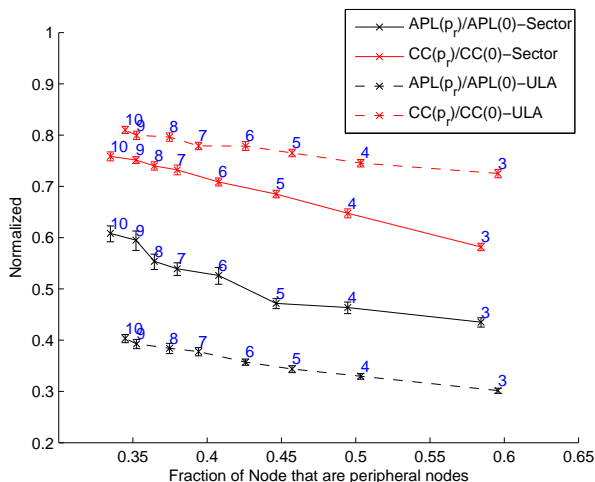


Fig. 14. Normalized *APL* and the *CC* for $N = 625$ showing the effects of the gradient for both the Sector and the ULA model.

However, for a low-density network, the algorithm reaches this consensus quickly.

VI. USEFUL CONCEPTS AND RELATED WORK

In this section, we define useful concepts giving an overview of the related work. We first define small world concepts in the section VI-A which form the basis of our research. The need of having long range links for achieving small world properties lead us to discuss beamforming in the section VI-B. We then define Lateral Inhibition in the section VI-C and Flocking in the section VI-D. The definitions of centrality concepts are discussed in the section VI-E. Further, we discuss non-uniform deployment in the section VI-F.

A. Small World Network

Inspired by Stanley Milgram's [3] experiment of "six degrees of separation", Watts et al [4] suggested a model for the creation of small world network. Watts et al in [4], [5] showed that rewiring edges of a regular network with a probability p_r results into reduction in the *APL* of the network while there is very little change in the *CC*. Starting by choosing a random vertex and one of its edge to the vertex's 1 hop neighbor with p_r , Watts et al reconnected the edge to a random vertex in the remaining network. Watts et al then considered all other vertices for rewiring. The process of rewiring continued with the edges now connecting the two hop neighbors. This process continued until all the edges were considered. p_r highly affected the rewiring process. Probability $p_r = 0$ meant that no rewiring while $p_r = 1$ meant complete rewiring of the graph. Using $p_r = 1$ resulted into complete randomness in the network.

The small world model motivated many research studies, [13], [6], [45], [7], and many models were proposed. Newman, [46], [8], compiled a comprehensive list of the models on small world. Mostly, the researchers studied two kinds of network structures, one without network growth while another with the network growth. Researchers analyzed the scaling and performance issues for the growing networks [6], [7]. Barabasi et al in [45], [7] showed that small world properties also exists in a growing network and there is a *preferential attachment* of the nodes giving rise to "rich gets richer" property. Barabasi et al showed that the real world networks possess these properties. This led to the behavioral analysis of the networks. On the contrary, assuming spatial wireless ad hoc network without growth, Helmy [13] performed the small world analysis and showed that rewiring of links does not change the structure of the network. Two other results shown in [13] are significant in the context of this paper. First, the *APL* is reduced at a greater rate when shortcuts are 25% to 40% in length of the network diameter. Second, the rate of the *APL* reduction is more when there are only 0.2% to 2% shortcut links. The reduction rate stabilizes when there are more than 2% shortcut links.

B. Antenna Model and Beamforming

Authors of [47], [48] provided an extensive study of antenna models and defined antenna gain using radiation intensity $u(\theta, \phi)$ where angle θ is angle with the z -axis and ϕ with the xy -plane as

$$g(\theta, \phi) = \frac{u(\theta, \phi)}{\frac{1}{4\pi} \int_0^{2\pi} \int_0^\pi u(\theta, \phi) \sin\theta d\theta d\phi} \quad (4)$$

Considering m antenna elements and isotropic radiators with same phase shift between them, researchers defined two basic antenna models Uniform Linear Array antenna model (*ULA*), (Cf. Fig. 15), and Uniform Circular Array antenna model (*UCA*). When $m = 1$, there is no superimposition of the radiation. This leads to a beam with omnidirectional characteristics.

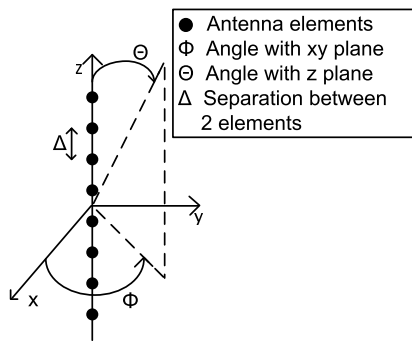


Fig. 15. Source: [47], Arrangement of $m = 8$ antenna elements in ULA model.

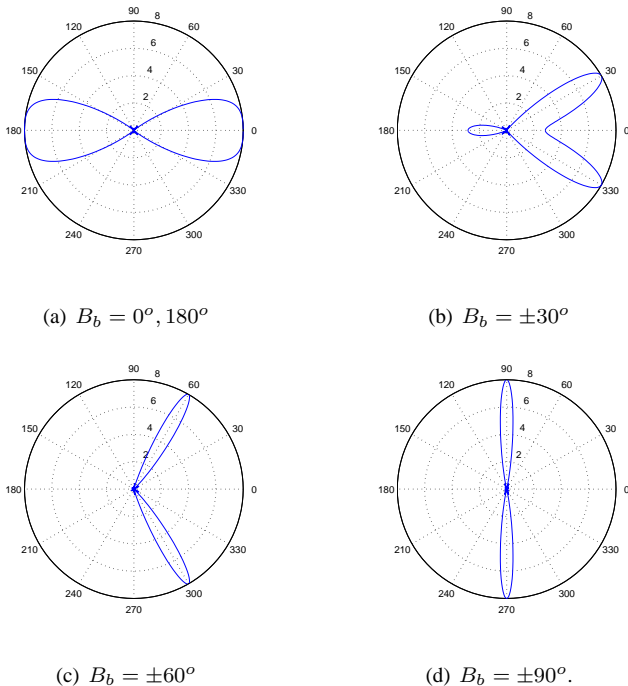


Fig. 16. Source: [47], Gain pattern obtained for different B_b and $m = 8$ in the ULA model

However, when $m > 1$, there is a constructive and destructive superimposition of the radiation due to the phase shift between the antenna elements. This leads to a beam with directional characteristics.

The gain pattern for the ULA antenna model is only dependent on the number of antenna elements. It has no dependency on the boresight direction (B_b , the direction of maximum radiation intensity, Cf. Fig. 16). On the other hand, for the UCA antenna model, gain pattern is dependent on both the number of antenna elements and B_b .

However, in wireless ad hoc networks, beamforming using UCA model has been well studied. Classical beamforming techniques using UCA model include Random Direction Beamforming (RDB) [47], [49], [50] and beamforming based on the angle of incidence and packet flow. Bettstetter et al [47] studied the use of RDB with the path probability to improve the connectivity in the wireless networks. Vilmann et al [51] derived low complexity techniques for beamforming and proposed Maximum Node Degree Beamforming (MNDB). In MNDB the nodes directed their beams towards the node that had maximum degree. The authors found that MNDB leads to

less number of inter-cluster connections but had more intra-cluster connections. To overcome this drawback, the authors proposed Two-hop Node Degree Beamforming (TNDB). In TNDB the nodes directed their beams towards the node that had maximum two-hop neighborhood. The authors showed that TNDB outperforms both RDB and MNDB. Other works on beamforming include [51], [52], [25], [53]. However, most of these studies were concentrated on nodes that were uniformly distributed at random in the given area but very few among them talk about non-uniform distribution of the nodes. Considering all nodes use directional beams, [47], [49], [51], [52], [25], [53] addressed connectivity very well but do not discuss the impact on the APL and the CC. Table II illustrates a comparison between these studies. On the other hand, studies related to the small world properties lack connectivity analysis for the non-uniformly distributed network. Table III illustrates comparisons between various studies performed in the direction of achieving small world properties in wireless ad hoc networks and our model.

C. Lateral Inhibition

Lateral Inhibition is a process by which cells of animal tissues, based on the properties of neighbor cells, decide whether to perform a task or not. Lateral Inhibition ensures that the cells that perform the tasks are equidistant from each other. This helps in producing regular patterns throughout the surface. Lawrence [19] modeled Lateral Inhibition as, when a cell performs a task, it inhibits its neighbors within h hops from performing that task thereby resulting into equally spaced uninhibited cells. Lateral Inhibition thus creates clusters where the cluster heads are uninhibited nodes distributed over an area. Nagpal et al [20], [21] described a simple algorithm to achieve Lateral Inhibition. In the algorithm, the cells assign themselves a random number. Each cell starts to count backwards. If before reaching 0, a node receives an inhibition signal from the neighboring cell, the cell stops counting otherwise sends out an inhibition signal to all its neighbors. Nagpal et al [20], [21] showed that the hopcount used to create the cluster greatly affects the number of clusters formed.

Recent studies revealed that Lateral Inhibition can be achieved in an optimal way [22]. Inspired by the tissue of the fruit fly, Afek et al [22] modeled distributed Lateral Inhibition using local information and requiring only two exchange mechanisms. These exchange mechanisms are, first, broadcasting a single control bit to the neighbors with certain probability and second, if the node receives no message from the neighbors, it sends out a control bit to inhibit its neighbors. As a variation to Nagpal et al's algorithm, the algorithm used a probabilistic approach that varied over time in an increasing manner to perform Lateral Inhibition. The runtime complexity of the algorithm was of the order $O(\log^2 |V|)$ where $|V|$ was the number of nodes in the system. Due to single bit exchange messages over single hop, the algorithm had a low message complexity.

D. Flocking

Flocking, [23], was first modeled by Reynolds in order to simulate the birds' behavior. In nature, flocking is observed in many other social living organisms like cattle, fishes and humans. Reynolds, while modeling Flocking, termed each social entity as a *boird* and formulated three very simple rules, (a) Alignment (b) Separation and (c) Cohesion. Reynolds defined Alignment rule as the direction matching of a *boird* with its neighbors. He defined Separation rule as the collision avoidance with neighborhood *boirds* and Cohesion rule as the tendency of a *boird* to remain as close to its neighbors as possible and not stray. The Fig. 17(a), shows that the *boird* orients itself in the direction in which its neighbors were moving. The Fig. 17(b), shows that the *boird* has to move away from the neighbors in order to avoid collision while

Parameter\ Reference	Vilzmann et al [49]	Widmer et al [51]	Kiese et al [52]	Yu et al [25]	Li et al [53]
Transmission mode	Directional	Directional	Directional	Directional	Both
Reception mode	Directional	Directional	Directional	Omnidirectional	Both
Mobility	No	Yes	No	No	No
Beam width	Depends on beam direction	Constant	Constant	Optional	Constant, switched beam antenna
Beam direction	Random	Optional	Optional	Optional	Random
Antenna model	UCA	UCA	UCA modeled as keyhole	Sector	Keyhole
Node distribution	Uniform	Uniform and Non-Uniform	Non-Uniform	Not specified	Uniform

TABLE II

COMPARISON BETWEEN VARIOUS STUDIES IN THE DIRECTION OF BEAMFORMING THAT FOCUS ON CONNECTIVITY. DUE TO EXTENSIVE LITERATURE, WE ONLY CONSIDER A LIMITED SET OF RESEARCH STUDIES HERE.

Parameter\ Reference	Our Model	Banerjee et al [18]	Guidoni et al [12]	Helmy et al [13]	Sharma et al [17]	Verma et al [54]
Shortcut Creation	Rewiring	Rewiring	Addition	Addition	Addition	Addition
Node distribution	Non-Uniform	Uniform	Uniform	Uniform	Uniform	Uniform
External infrastructure	No	No	High range Sensor	-	Wired	Two radios for each node
Global knowledge	No	No	Yes	Yes	Yes	Yes
Density of nodes	Low	High	High	High	-	Low
Shortcut Edge	Directed	Directed	Undirected	Undirected	Undirected	Directed
Shortcut direction	Towards centroid of other region	Longest Traffic Flow path	Random, towards sink	Random	Random	Random
Shortcut length	Function of antenna elements	Function of node density	Constant	Limited	Constant	Constant
Shortcut width	Depends on Shortcut Length	Depends on Shortcut Length	Constant	-	-	Constant
Prob. of Shortcut creation	(0, 1] based on model parameters	Based on centrality values	$\in (0, 1]$	$\in (0, 1]$	function of network size	$\in (0, 1]$
Performance metric	Path length, Clust. Coeff. Connectivity	Path length, Connectivity	Path length, Clust. Coeff.	Path length, Clust. Coeff.	Path length, Energy	Path length, Clust. Coeff., degree

TABLE III

COMPARISON BETWEEN VARIOUS RESEARCH STUDIES IN THE DIRECTION OF ACHIEVING SMALL WORLD PROPERTIES IN THE WIRELESS AD HOC NETWORKS. OTHER RESEARCH STUDIES IN THIS DIRECTION CONSIDER USE OF EXTERNAL INFRASTRUCTURE OF AT LEAST TWO RADIOS.

the Fig. 17(c) shows that the *boird* moves towards the centroid of the neighbors in order to remain close to its neighborhood. Couzin in [55] formulated mathematical explanation of these rules. Due to the motion of a *boird*, velocity and displacement were associated with the *boird*. Alignment rule was modeled using the direction of a *boird* while Separation and Cohesion were modeled using both velocity and the displacement.

Recent studies have revealed the use of Flocking in solving various problems in wireless ad hoc networks. Antoniou et al [56] used Flocking to provide efficient congestion control mechanism by computing the congestion at the neighbor nodes while [57] used the Separation rule for the efficient placement of nodes to maximize the coverage area.

E. Centrality

Decades of research on network and graph theory has led researchers to derive many fundamental concepts related to the importance of a node in the network. The concept of centrality was one such concept that was developed and used to address the topological characteristics of the network nodes. Proposed definitions of centrality measures include those that use global parameters as well as those that only use local information. Some examples of global centrality measures are Socio-Centric Betweenness [28], [29] and Closeness Centrality [28] while Degree

Centrality [28] and Egocentric Betweenness Centrality [58], [59] are examples of the local centrality measure.

1) *Socio-Centric Betweenness Centrality*: The Socio-Centric Betweenness Centrality, [28], [29], is the measure of the number of shortest paths passing through the node thereby expressing the most important node in the network and through which most of the communication takes place. The Socio-Centric Betweenness is a frequency measure and requires the global network knowledge. Usually nodes with high degree and those that are acting as the bridge nodes tend to have relatively high Socio-Centric Betweenness. Mathematically the Socio-Centric Betweenness of a node v is

$$BC_v = \sum \frac{sp(v)}{sp} \quad (5)$$

where $sp(v)$ is the number of shortest paths between any two nodes that pass through v while sp is the total number of shortest paths in the network.

2) *Egocentric Betweenness Centrality*: Aiming to compute the Betweenness centrality using local properties, [58], [59] proposed the Egocentric Betweenness Centrality measure. Everett in [58] computed the Egocentric Betweenness using upper diagonal adjacency matrix A_v . A_v is created considering 1 hop neighborhood of the node v . Consider I to be the identity matrix,

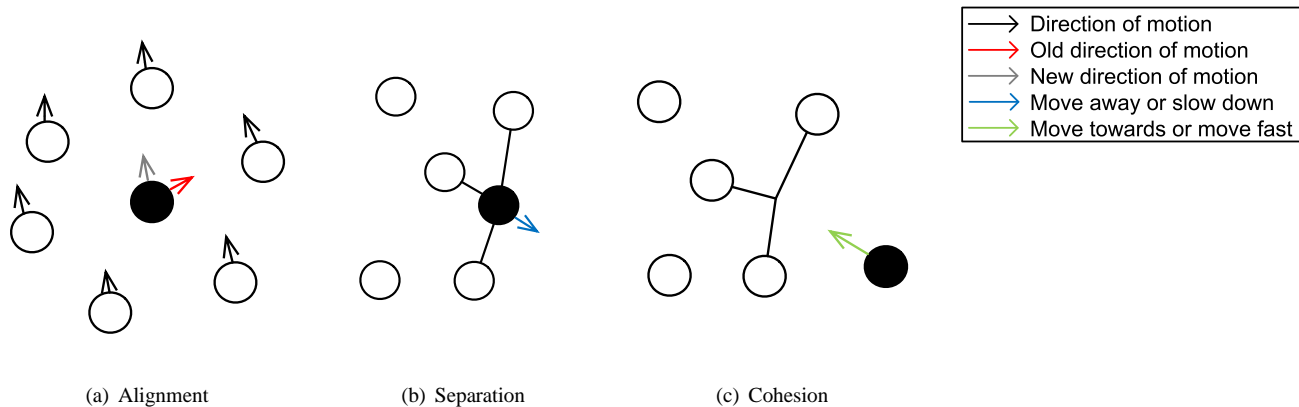


Fig. 17. Source: [23], Depiction of three Flocking rules.

then the sum of the inverse of all non-zero elements in A_v^2 along $[I - A_v]$ is the Egocentric Betweenness of the node.

Marsden in [42] performed an empirical study to find the relation between the two types of Betweenness, the Socio-Centric and the Egocentric Betweenness, and found that the Egocentric Betweenness is strongly correlated to the Socio-Centric Betweenness and it can be used when global network information is lacking.

3) *Closeness Centrality*: The Closeness Centrality [28] on the other hand is the measure of how fast a node can transfer data to all the nodes. The Closeness Centrality is the fraction of shortest distance between a node to all other nodes in the network. Assuming $sd(v, w)$ be the shortest distance between node v and w , the Closeness Centrality of v is

$$C_v = \frac{1}{\sum_{w \neq v, w \in V} sd(v, w)} \quad (6)$$

A node with the highest Closeness Centrality value is the centroid of the network.

As all the centrality measures convey different information, it is not necessary that a node having high value for one centrality measure also have high values for the others. Many other types of centralities, such as, Bridging Centrality, Eigen Vector Centrality and Spectral Centrality also exist. We refrain ourselves from describing them in detail. However, Katsaros, [60], provided a brief survey on these centrality measures.

F. Non-Uniform distribution of nodes

Many non-uniform deployment strategies have been proposed, [61], [62], [63], [64], [65], [24]. We take insights from Bettstetter et al, [24], node deployment strategy. Bettstetter et al proposed the use of thinning process to generate a non-uniform node deployment. The authors started with uniform distribution of nodes in a given region, then pruned the nodes based on two factors, transmission radius, r_b , and the number of neighbor nodes, ℓ_{min} . If the node had at least ℓ_{min} neighbors within r_b , the node was not removed else it was removed. Schilcher et al, [66], formulated and measured the degree of non-uniformity of this pruned network. Schilcher et al divided the region into smaller sub-regions and estimated the number of nodes in the sub-region. The estimated value was then used to calculate the non-uniformity index, $hIndex$. The Fig. 18(b) shows the deployment achieved when the thinning process is applied to the deployment shown by the Fig. 18(a). The Fig. 18(c) shows the density distribution of nodes using kernel method.

VII. FUTURE WORK

A Number of extensions to our algorithm can be visualized. Identifying the optimal gradient size to choose for the

determination of minimal peripheral set of nodes is one way of extending our work. We are currently working on how we can apply game theory to successfully find the minimal peripheral set. We believe that by applying game theory nodes can determine what the suitable gradient size is and can reduce asymmetric links further.

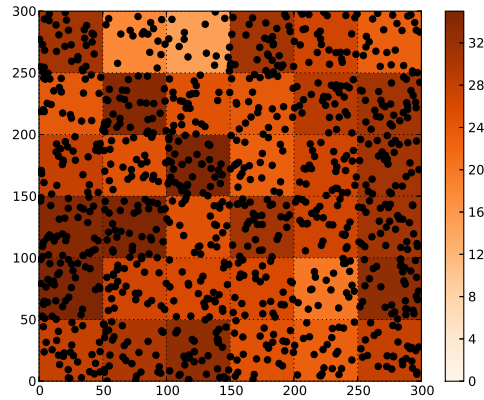
We would also like to extend our algorithm to support dynamic environment and asynchronous operation. Dynamic environments are likely to result in frequent changes to the state of the node. Any change in the state of the node would require reconfiguring in the network using the proposed algorithm. Information available at the neighborhood nodes would be helpful in learning about the previous configuration. This learning could be *docitive* [67], meaning, partial learning from the neighborhood states could make nodes infer about the previous good configuration so that reconfiguration can be done easily and quickly. This will also help us to address the unaddressed paradigms of [27]. Further, we would like to address network lifetime of the network when implementing our algorithm.

VIII. CONCLUSION

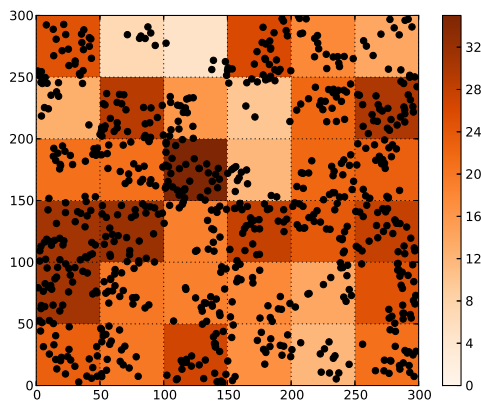
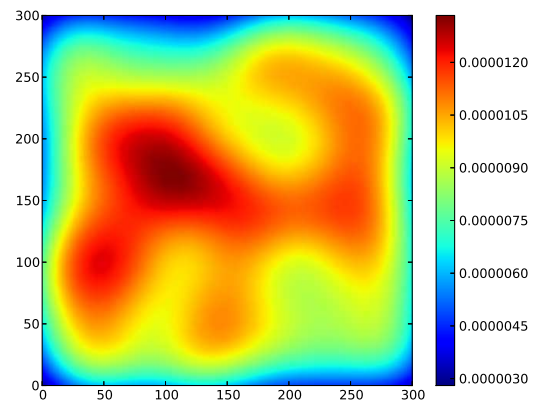
In this paper, we have presented an algorithm for achieving small world properties using beamforming and bio-inspired techniques in a wireless ad hoc network. Our algorithm works using locally available information and does not require the knowledge of the network. We have also removed the possibility of requirement of any external infrastructure for achieving our goal. Through our algorithm, we have shown how isolated communities can collaborate and connect with each other to achieve better and faster communication. Bio-Inspired techniques like Lateral Inhibition helped us to form communities within the network for the reduced message complexity while the Flocking analogy helped us to determine beam properties. Our results show that for both theoretical and realistic antenna models and relatively high-density networks, there is a reduction in the *APL* by almost 40% to 68% for $g \in [3, 10]$. On the other hand, reduction in the *CC* is between 19% to 38%. Our results also show improvement in the connectivity. The increase in the size of the *GSCC* for the non-uniformly distributed directional network is around 10% for high density network while it is around 61% for relatively low density networks.

REFERENCES

- [1] I. Akyildiz and I. Kasimoglu, "Wireless Sensor and Actor Networks: Research Challenges," *Ad Hoc Networks*, vol. 2, pp. 351–367, Oct 2004.
- [2] F. Dressler, *Self-Organization in Sensor and Actor Networks*. Chichester, UK: John Wiley & Sons, Nov 2007.



(a) Uniform node distribution with the node density.

(b) Distribution after applying the Thinning process with $r_b = 15$ and $\ell_{min} = 6$ on the distribution as in the Fig. 18(a).

(c) Distribution pattern using Kernel method for the Fig. 18(b).

Fig. 18. Node Distribution.

- [3] J. Travers and S. Milgram, “An Experimental Study of the Small World Problem,” *Sociometry*, vol. 32, pp. 425–443, Dec 1969.
- [4] D. J. Watts and S. Strogatz, “Collective Dynamics of Small World Networks,” *Nature*, vol. 393, pp. 440–442, June 1998.
- [5] D. J. Watts, *Small Worlds: The Dynamics of Networks between Order and Randomness*. New Jersey: Princeton University Press, 2003.
- [6] A. L. Barabási and E. Bonabeau, “Scale-Free Networks,” *Scientific American*, vol. 288, pp. 60–69, May 2003.
- [7] A. L. Barabási and R. Albert, “Emergence of Scaling in Random Networks,” *Science*, vol. 286, pp. 509–512, Oct 1999.
- [8] M. E. J. Newman, “The Structure and Function of Complex Networks,” *SIAM Review*, vol. 45, no. 2, pp. 167–256, 2003.
- [9] M. Brust and S. Rothkugel, “Small Worlds: Strong Clustering in Wireless Networks,” in *Proceedings of 1st International Workshop on Localized Algorithms and Protocols for Wireless Sensor Networks*, (Santa Fe, NM), pp. 78–86, IEEE, New York, 18-20 June 2007.
- [10] J. Kleinberg, “The Small World Phenomenon: An Algorithm Perspective,” in *Proceedings of the 32nd Annual ACM Symposium on Theory of Computing*, (Portland, OR), pp. 163–170, ACM, New York, 21-23 May 2000.
- [11] R. Albert, H. Jeong, and A. L. Barabasi, “Error and Attack Tolerance of Complex Networks,” *Nature*, vol. 406, pp. 378–382, July 2000.
- [12] D. Guidoni, R. Mini, and A. Loureiro, “On the Design of Resilient Heterogeneous Wireless Sensor Networks Based on Small World Concepts,” *Computer Networks*, vol. 54, pp. 1266–1281, June 2010.
- [13] A. Helmy, “Small Worlds in Wireless Networks,” *IEEE Communications Letters*, vol. 7, no. 10, pp. 490–492, 2003.
- [14] H. A. Simon, “On a Class of Skew Distribution Functions,” *Biometrika*, vol. 42, no. 3-4, pp. 425–440, 1955.
- [15] M. Barthélemy, “Crossover from Scale-Free to Spatial Networks,” *Europhysics Letters*, vol. 63, pp. 915–921, Sept 2003.
- [16] S. Manna and P. Sen, “Modulated Scale-Free Network in Euclidean Space,” *Physical Review E*, vol. 66, pp. 1–4, dec 2002.
- [17] G. Sharma and R. Mazumdar, “A Case for Hybrid Sensor Networks,” *IEEE/ACM Transaction on Networking*, vol. 16, no. 5, pp. 1121–1132, 2008.
- [18] A. Banerjee, R. Agarwal, V. Gauthier, C. K. Yeo, H. Afifi, and B. S. Lee, “Self-Organization of Wireless Ad Hoc Networks as Small Worlds using Long Range Directional Beams,” in *Proceedings of IEEE GLOBECOM Workshop on Complex Communication Networks (CCNet)*, (Houston, TX), pp. 120–124, IEEE, New York, 5-9 December 2011.
- [19] P. Lawrence, “The Making of a Fly: The Genetics of Animal Design,” *Molecular Reproduction and Development*, vol. 37, pp. 120–120, Jan 1994.
- [20] R. Nagpal and D. Coore, “An Algorithm for Group Formation in an Amorphous Computer,” in *Proceedings of International Conference of Parallel and Distributed Systems*, (Las Vegas, NV), pp. 1–4, IASTED Press, Calgary, Canada, 1-4 October 1998.
- [21] R. Nagpal and M. Mamei, “Engineering Amorphous Computing Systems,” in *Methodologies and Software Engineering for Agent Systems* (F. Bergenti, M. P. Gleizes, F. Zambonelli, and G. Weiss, eds.), vol. 11 of *Multiagent Systems, Artificial Societies, and Simulated Organizations*, pp. 303–320, Boston: Springer, 2004.
- [22] Y. Afek, N. Alon, O. Barad, E. Hornstein, N. Barkai, and Z. Bar-

- Joseph, "A Biological Solution to a Fundamental Distributed Computing Problem," *Science*, vol. 331, pp. 183–185, Jan 2011.
- [23] C. Reynolds, "Flocks, Herds and Schools: A Distributed Behavioral Model," *ACM SIGGRAPH Computer Graphics*, vol. 21, pp. 25–34, July 1987.
- [24] C. Bettstetter, M. Gyarmati, and U. Schilcher, "An Inhomogeneous Spatial Node Distribution and its Stochastic Properties," in *Proceedings of the 10th ACM Symposium on Modeling, Analysis, and Simulation of Wireless and Mobile Systems*, (Chania, Greece), pp. 400–404, ACM, New York, 22–26 October 2007.
- [25] Z. Yu, J. Teng, X. Bai, D. Xuan, and W. Jia, "Connected Coverage in Wireless Networks with Directional Antennas," in *Proceedings of IEEE International Conference on Computer Communications*, (Shanghai, China), pp. 2264–2272, IEEE, New York, 10–15 April 2011.
- [26] UM-CS-2010-066, "Efficient Algorithms for Neighbor Discovery in Wireless Networks," tech. rep., University of Massachusetts, Amherst, MA, 2010.
- [27] Z. Prehofer and C. Bettstetter, "Self-Organization in Communication Networks: Principles and Design Paradigms," *Communications Magazine, IEEE*, vol. 43, pp. 78–85, July 2005.
- [28] L. C. Freeman, "Centrality in Social Networks Conceptual Clarification," *Social Networks*, vol. 1, no. 3, pp. 215–239, 1979.
- [29] L. C. Freeman, "A Set of Measures of Centrality Based on Betweenness," *Sociometry*, vol. 40, no. 1, pp. 35–41, 1977.
- [30] M. R. Brust, C. H. C. Ribeiro, D. Turgut, and S. Rothkugel, "LSWTC: A Local Small World Topology Control Algorithm for Backbone-Assisted Mobile Ad Hoc Networks," in *Proceedings of 35th Conference on Local Computer Network*, (Denver, CO), pp. 144–151, IEEE, New York, 10–14 October 2010.
- [31] M. Brust, A. Andronache, and S. Rothkugel, "WACA: A Hierarchical Weighted Clustering Algorithm Optimized for Mobile Hybrid Networks," in *Proceedings of 3rd International Conference on Wireless and Mobile Communication*, (Guadeloupe, French Caribbean), pp. 23–30, IEEE, Washington DC, 4–9 March 2007.
- [32] W. Heinzelman, A. Chandrakasan, and H. Balakrishnan, "An Application-Specific Protocol Architecture for Wireless Micro-Sensor Networks," *IEEE Transaction on Wireless Communication*, vol. 1, pp. 660–670, Oct 2002.
- [33] O. Younis and S. Fahmy, "HEED: A Hybrid, Energy-Efficient, Distributed Clustering Approach for Ad Hoc Sensor Networks," *IEEE Transactions on Mobile Computing*, vol. 3, pp. 366–379, Oct 2004.
- [34] S. Capkun, M. Hamdi, and J. P. Hubaux, "GPS-Free Positioning in Mobile Ad Hoc Networks," in *Proceedings of the 34th Annual Hawaii International Conference on System Sciences*, (Wailea Maui, Hawaii), pp. 1–10, IEEE, New York, 3–6 January 2001.
- [35] A. Caruso, S. Chessa, S. De, and A. Urpi, "GPS Free Coordinate Assignment and Routing in Wireless Sensor Networks," in *Proceedings of 24th Annual Joint Conference of the IEEE Computer and Communications Societies*, vol. 1, (Miami, FL), pp. 150–160, IEEE, New York, 13–17 March 2005.
- [36] B. Leong, B. Liskov, and R. Morris, "Greedy Virtual Coordinates for Geographic Routing," in *Proceedings of IEEE International Conference on Network Protocols (ICNP)*, (Beijing, China), pp. 71–80, IEEE, New York, 16–19 October 2007.
- [37] F. Dabek, R. Cox, F. Kaashoek, and R. Morris, "Vivaldi: A Decentralized Network Coordinate System," *ACM SIGCOMM Computer Communication Review*, vol. 34, pp. 15–26, Aug 2004.
- [38] A. Rao, S. Ratnasamy, C. Papadimitriou, S. Shenker, and I. Stoica, "Geographic Routing without Location Information," in *Proceedings of 9th Annual International Conference on Mobile Computing and Networking*, (San Diego, CA), pp. 96–108, ACM, New York, 16–19 September 2003.
- [39] 892, "Anchor-Free Distributed Localization in Sensor Networks," tech. rep., MIT Laboratory for Computer Science, Boston, MA, 2003.
- [40] T. Watteyne, I. Augé-Blum, M. Dohler, S. Ubéda, and D. Barthel, "Centroid Virtual Coordinates: A Novel Near-Shortest Path Routing Paradigm," *Computer Networks*, vol. 53, pp. 1697–1711, July 2009.
- [41] A. Awad, R. German, and F. Dressler, "Exploiting Virtual Coordinates for Improved Routing Performance in Sensor Networks," *IEEE Transactions on Mobile Computing*, vol. 10, pp. 1214–1226, Sept 2011.
- [42] P. Marsden, "Egocentric and Sociocentric Measures of Network Centrality," *Social Networks*, vol. 24, pp. 407–422, Oct 2002.
- [43] E. Ravasz and A. L. Barabasi, "Hierarchical Organization in Complex Networks," *Physical Review E*, vol. 67, pp. 1–7, Dec 2002.
- [44] S. Dorogovtsev, J. Mendes, and A. Samukhin, "Giant Strongly Connected Component of Directed Networks," *Physical Review E*, vol. 64, pp. 025101–025104, Jul 2001.
- [45] R. Albert, H. Jeong, and A. L. Barabasi, "The Diameter of the World Wide Web," *Nature*, vol. 401, pp. 130–131, 1999.
- [46] M. E. J. Newman, "Models of the Small World: A Review," *Journal of Statistical Physics*, vol. 101, pp. 819–841, November 2000.
- [47] C. Bettstetter, C. Hartmann, and C. Moser, "How does Randomized Beamforming Improve the Connectivity of Ad Hoc Networks?," in *Proceedings of the IEEE International Conference on Communications (ICC)*, vol. 05, (Seoul, Korea), pp. 3380–3385, IEEE, New York, 16–20 May 2005.
- [48] C. Balanis, *Antenna Theory-Analysis and Theory*. New York: Wiley, 1997.
- [49] R. Vilmann, C. Bettstetter, D. Medina, and C. Hartmann, "Hop Distances and Flooding in Wireless Multihop Networks with Randomized Beamforming," in *Proceedings of the 8th International Symposium on Modeling, Analysis and Simulation of Wireless and Mobile systems*, (Montreal, Canada), pp. 20–27, ACM, New York, 10–13 October 2005.
- [50] R. Vilmann, C. Bettstetter, and C. Hartmann, "BeamMAC: A new Paradigm for Medium Access in Wireless Networks," *AEU - International Journal of Electronics and Communications*, vol. 60, pp. 3–7, Jan 2006.
- [51] R. Vilmann, J. Widmer, I. Aad, and C. Hartmann, "Low Complexity Beamforming Techniques for Wireless Multihop Networks," in *Proceedings of 3rd Annual IEEE Communication Society on Sensor and Ad Hoc Communication and Networks*, (Reston, VA), pp. 489–497, IEEE, New York, 25–28 September 2006.
- [52] M. Kiese, C. Hartmann, J. Lamberty, and R. Vilmann, "On Connectivity Limits in Ad Hoc Networks with Beamforming Antennas," *EURASIP Journal on Wireless Communication and Networks*, vol. 2009, pp. 1–15, 2009.
- [53] P. Li, C. Zhang, and Y. Fang, "Asymptotic Connectivity in Wireless Ad Hoc Networks Using Directional Antennas," *IEEE/ACM Transaction on Networking*, vol. 17, pp. 1106–1117, Aug 2009.
- [54] C. K. Verma, B. R. Tamma, B. S. Manoj, and R. Rao, "A Realistic Small World Model for Wireless Mesh Networks," *Communications Letters, IEEE*, vol. 15, pp. 455–457, April 2011.
- [55] I. D. Couzin, J. Krause, N. R. Franks, and S. A. Levin, "Effective Leadership and Decision-Making in Animal Groups on the Move," *Nature*, vol. 433, pp. 513–516, Feb 2005.
- [56] P. Antoniou, A. Pitsillides, A. Engelbrecht, T. Blackwell, and L. Michael, "Congestion Control in Wireless Sensor Networks Based on the Bird Flocking Behavior," in *Proceedings of the 4th IFIP TC 6 International Workshop on Self-Organizing Systems*, (Zurich, Switzerland), pp. 220–225, Springer-Verlag, Berlin, 9–11 December 2009.
- [57] B. A. Kadrovach and G. B. Lamont, "A Particle Swarm Model for Swarm-Based Networked Sensor Systems," in *Proceedings of ACM Symposium on Applied Computing*, (Madrid, Spain), pp. 918–924, ACM, New York, 11–14 March 2002.
- [58] M. Everett and S. Borgatti, "Ego Network Betweenness," *Social Networks*, vol. 27, pp. 31–38, Jan 2005.
- [59] E. Daly and M. Haahr, "Social Network Analysis for Routing in Disconnected Delay-Tolerant MANETs," in *Proceedings of 8th ACM International Symposium on Mobile Ad Hoc Networking and Computing*, (Montreal, Canada), pp. 32–40, ACM, New York, 9–14 September 2007.
- [60] D. Katsaros, N. Dimokas, and L. Tassioulas, "Social Network Analysis Concepts in the Design of Wireless Ad Hoc Network Protocols," *Network*, vol. 24, pp. 23–29, Nov–Dec 2010.
- [61] W. Hsu, T. Spyropoulos, K. Psounis, and A. Helmy, "Modeling Time-Variant User Mobility in Wireless Mobile Networks," in *Proceedings of 26th IEEE International Conference on Computer Communications*, (Anchorage, AK), pp. 758–766, IEEE, New York, 6–12 May 2007.
- [62] J. Y. Le Boudec and M. Vojnovic, "The Random Trip Model: Stability, Stationary Regime, and Perfect Simulation," *IEEE/ACM Transactions on Networking*, vol. 14, pp. 1153–1166, Dec 2006.
- [63] L. Hu and L. Dittmann, "Heterogeneous Community-Based Mobility Model for Human Opportunistic Network," in *Proceedings of the 2009 IEEE International Conference on Wireless and Mobile Computing, Networking and Communications*, (Marrakech, Morocco), pp. 465–470, IEEE, New York, 12–14 October 2009.

- [64] N. Aitsaadi, N. Achir, K. Boussetta, and G. Pujolle, "Artificial Potential Field Approach in WSN Deployment: Cost, QoM, Connectivity and Lifetime Constraints," *Computer Networks*, vol. 55, pp. 84–105, Jan 2011.
- [65] J. Riihijarvi, M. Petrova, and P. Mahonen, "Influence of Node Location Distributions on the Structure of Ad Hoc and Mesh Networks," in *Proceedings of Global Telecommunications Conference*, (New Orleans, LO), pp. 1–5, IEEE, New York, 28 Nov-30 Dec 2008.
- [66] U. Schilcher, M. Gyarmati, C. Bettstetter, Y. W. Chung, and Y. H. Kim, "Measuring Inhomogeneity in Spatial Distributions," in *Proceedings of Vehicular Technology Conference*, (Singapore), pp. 2690–2694, IEEE, New York, 11-14 May 2008.
- [67] L. Giupponi, A. Galindo-Serrano, P. Blasco, and M. Dohler, "Dognitive Networks: An Emerging Paradigm for Dynamic Spectrum Management [Dynamic Spectrum Management]," *Wireless Communications, IEEE*, vol. 17, pp. 47–54, August 2010.